

Integrated Master in Chemical Engineering

Synthesis of nanostructured Ni(Co)/C/SiO₂ composites from cellulose derivatives through sol-gel approach

Master Thesis

Development Project in a Foreign Institution

Joana Filipa Fernandes Valente Baldaia



Universidade do Porto
Faculdade de Engenharia
FEUP

Department of Chemical Engineering



CHALMERS

Department of Microtechnology and Nanoscience

MC2

Examiner: Peter Enoksson

Supervisor: Olga Naboka

Evaluator in the home institution: José Luís Figueiredo

July 2012

The carbon age: dark element, brighter future.

Aaron Feaver [1]

Acknowledgments

At the end of my master thesis I would like to thank all special people who made this thesis possible and an unforgettable experience for me.

A special thanks to my supervisor, Olga Naboka. This work would not have been possible without her guidance, support and encouragement. Thanks for the knowledge transmitted and for answering, with a lot of patience my questions and doubts. There are not enough words to describe your excellent work in this group and your admirable supervision.

I am extremely grateful to my examiner Professor Peter Enoksson for the opportunity to work in his group and for providing meetings and resources to accomplish my research work.

The results described in this thesis would have been obtained with a close collaboration with WWSC and I owe a great deal of appreciation to Professor Paul Gatenholm.

Thanks to Professor José Luís Figueiredo, my evaluator in FEUP, for the detailed evaluation about the work developed.

I am thankful to Volodymyr Kuzmenko for his precious recommendation and his discussions about my work. Thanks also to all people in MNS group and People in 8th floor of chemistry building.

I will be always grateful to my best flat partner and friend Filipa during these strong 5 months. Thanks for hear all my complaints sometimes almost 24 hours a day and for helpful criticism. I am sure that I will miss her.

A special thanks to Timóteo for the wonderful week we spent together in Sweden, which made him an excellent source of inspiration.

I expand my thanks to Celine, Jessica, Russol, João, Nuno, Miguel, Daniel, Jorge who shared their incredibly varied life experiences with me during my stay in Sweden, and extended friendship towards me.

My last thanks but definitely not the least, go to my family members especially my father, my mother and my brother who helped me emotionally and materially to overcome all the obstacles I faced during these 5 months.

Abstract

Carbon nanostructured composites have gained a lot of interest, since they have unique chemical, physical, magnetic and mechanical properties. These materials have potential for a wide range of application as energy storage, catalysis, supercapacitors, sensors, drug delivery, ion exchange and separation processes.

The aim of this project was the synthesis of Ni(Co)/C/SiO₂ composites by sol-gel approach using cellulose acetate and hydroxypropyl cellulose as a carbon precursors and TEOS as silica precursor. These polymers were chosen as carbon precursors because of their renewability and low cost.

Synthesized materials were investigated with low-temperature nitrogen sorption, Scanning Electron Microscopy (SEM), X-Ray diffraction (XRD) and Thermal Gravimetric Analysis (TGA).

Micro-and mesoporous Ni(Co)/C/SiO₂ composites were synthesized by carbonization of precursor containing xerogels. Presence of metallic Ni and Co was proven with XRD.

Our study showed that the structure and properties of the nanocomposites synthesized are influenced by precursor and type of metal salt used. The use of cellulose acetate and cobalt bromide made it possible to prepare silica/carbon materials with surface area values up to 346 m² g⁻¹. results obtained could be explained with complex interactions between Ni(II) or Co(II) salt, precursor and silica in formed gels.

Keywords: cellulose acetate; hydroxypropyl cellulose, sol-gel process, carbonization, Ni(Co)/C/SiO₂ composites.

Resumo

Os compósitos nanoestruturados de carbono têm ganho muito interesse porque apresentam propriedades químicas, físicas, magnéticas e mecânicas únicas. Estes materiais têm potencial para uma larga escala de aplicações, como o armazenamento de energia, catálise, supercapacitores, sensores, troca iónica e processos de separação.

O objectivo deste projeto foi a síntese de compósitos de Ni(Co)/C/SiO₂ através do processo sol-gel usando acetato de celulose e hidroxipropilcelulose como precursor de carbono e TEOS como precursor de sílica. Estes polímeros foram selecionados como precursores de carbono porque são renováveis e apresentam baixo custo.

Os materiais sintetizados foram investigados por adsorção de azoto a baixa temperatura, microscopia de varrimento electrónico (SEM), difração de raios X (XRD) e análise térmica gravimétrica (TGA).

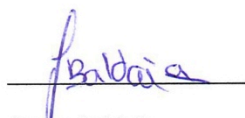
Foram sintetizados micro e mesoporos de Ni(Co)/C/SiO₂ através da carbonização do precursor contendo xerogéis. A presença de níquel e cobalto metálico foi provado por análise XRD.

Este estudo mostrou que a estrutura e as propriedades dos nanocompósitos sintetizados são influenciados pelo precursor e pelo tipo de metal usado. O uso de acetato de celulose e brometo de cobalto tornou possível a preparação de materiais de sílica/carbono com áreas superficiais até 346 m² g⁻¹. Estes resultados recebidos podem ser explicados com formação de complexos devido à interação dos metais Ni(II) e Co(II), do precursor de carbono e sílica para formação de géis.

Palavras chave: acetato de celulose, hidroxipropilcelulose, processo sol-gel, carbonização, compósitos de Ni(Co)/C/SiO₂.

Declaração

Declaro, sob compromisso de honra, que este trabalho é original e que todas as contribuições não originais foram devidamente referenciadas com identificação da fonte.

A handwritten signature in blue ink, appearing to read 'Baldaia', is written over a horizontal line.

Joana Baldaia

Göteborg, 9th July, 2012

Table of contents

List of Figures	iv
List of Tables	vii
List of Equations	viii
Abbreviations and symbols.....	ix
1 Problem Statement	1
1.1 Description of Project work plan.....	1
1.2 Overview of thesis.....	2
2 Background of the study.....	3
2.1 Porous carbon nanomaterials	3
2.1.1 Methods for the synthesis of porous carbon materials	3
2.1.2 Applications of carbon porous materials.....	5
2.2 Silica is promising template for the synthesis of carbon porous nanomaterials	7
2.3 Sol gel process.....	8
2.3.1 Formation of silica sol by hydrolysis of TEOS	9
2.3.2 Gelation.....	11
2.3.3 Ageing.....	11
2.3.4 Drying	11
2.3.5 Factors affecting the sol-gel process.....	11
i) Effect of Water-to-alkoxide molar ratio	11
ii) pH effect	12
2.4 Cellulose: fascinating biopolymer	13
2.4.1 Cellulose acetate.....	13
2.4.2 Hydroxypropyl cellulose.....	14
2.4.3 Carbonization of cellulose	14
2.5 Modification of properties of carbon materials with transitional metals.....	15

2.5.1	Cobalt	16
2.5.2	Nickel	16
3	Aim of the work	17
4	Materials and Methods	18
4.1	Synthesis of silica xerogels	18
4.1.1	Materials	18
4.1.2	Preparation of cellulose solutions	18
4.1.3	Preparation of metal salts solutions.....	18
4.1.4	Sol-Gel Process	18
i)	Sol-gel Reactions	18
ii)	Ageing	19
iii)	Drying	19
4.2	Synthesis of carbon nanocomposites	19
4.3	Characterization techniques	20
4.3.1	Specific surface area	20
4.3.2	Termo gravimetric analysis (TGA)	20
4.3.3	Scanning Electron Microscopy (SEM).....	21
4.3.4	X-ray Diffraction (XRD)	21
4.3.5	Fourier transform infrared spectroscopy (FTIR)	21
5	Results and discussion.....	22
5.1	Formation of precursor containing gels.....	22
5.1.1	Gels prepared in the presence of HPC	22
i)	Fourier transform infrared spectroscopy of carbon samples synthesized from HPC containing gels	22
5.1.2	Gels prepared in the presence of CA.....	24
i)	Fourier transform infrared spectroscopy of carbon samples synthesized from CA containing gels25	
5.2	Carbonization of precursor containing xerogels	28
5.2.1	Carbonization of HPC containing composites.	28

i) Low temperature nitrogen sorption isotherms of carbon composite samples synthesized from HPC containing gels.	29
ii) SEM of carbon samples synthesized from HPC containing gels.	31
iii) X-Ray Diffraction of carbon composite samples synthesized from HPC containing gels.....	32
5.2.2 Carbonization of CA containing composites.	33
i) Low temperature nitrogen sorption isotherms of carbon composite samples synthesized from CA containing gels.	33
ii) SEM images of carbon composite samples synthesized from CA containing gels.....	37
iii) X-Ray Diffraction of carbon composite samples synthesized from CA containing gels.	40
5.3 Discussion	42
6 Conclusions	43
6.1 Other work performed	43
6.2 Future work	44
6.3 Final appreciation	44
7 References	45
8 Appendix	49

List of Figures

Figure 1 Typical methods used for the synthesis of nanoporous materials [5]	4
Figure 2 Carbon electrode for battery applications [1]	6
Figure 3 'On the molecular origin of supercapacitance in nanoporous carbon electrodes'[13]	6
Figure 4 Diffusion path of lithium ions (Li+) through nanopores of a nanoporous active material [14].	6
Figure 5 Steps of the sol gel process	8
Figure 6 TEOS, H ₂ O and alcohol ternary phase diagram. For pure ethanol the miscibility line is shifted slightly to the right [16].	9
Figure 7 Silica matrix.....	10
Figure 8 Point-of-zero-charge (PZC) of silica [15].....	12
Figure 9 Chemical structure of cellulose acetate	13
Figure 10 chemical structure of hydroxypropyl cellulose.....	14
Figure 11 Scheme of cellulose decomposition during carbonization	15
Figure 12 a) The furnace in cleanroom b) powder samples in alumina crucibles after carbonization.	19
Figure 13 Gels formed in the presence of HPC - a: cobalt chloride, b: nickel chloride; c: without salt...	22
Figure 14 FTIR spectra for pure HPC	23
Figure 15 FTIR spectra for HPC/SiO ₂ composite.....	23
Figure 16 FTIR spectra for CoCl ₂ /HPC/SiO ₂ composite before carbonization.....	24
Figure 17 FTIR spectra for NiCl ₂ /HPC/SiO ₂ composite before carbonization	24
Figure 18 Gels formed in the presence of CA - a: cobalt bromide, b: cobalt bromide, c: nickel chloride.	25
Figure 19 FTIR spectra for pure CA	25
Figure 20 FTIR spectra for CA/SiO ₂ composite.....	26
Figure 21 FTIR spectra for CoCl ₂ /CA/SiO ₂ composite before carbonization.....	27
Figure 22 FTIR spectra for CoBr ₂ /CA/SiO ₂ composite before carbonization.....	27
Figure 23 FTIR spectra for Co(NO ₃) ₂ /CA/SiO ₂ composite before carbonization.	28
Figure 24 TGA of SG4 samples carbonized in powder and monolith condition.	29
Figure 25 Low temperature nitrogen sorption isotherms of carbon composite sample SG1 and SG2...	29
Figure 26 Low temperature nitrogen sorption isotherms of carbon composite sample SG3 and SG4...	29
Figure 27 Pore size distribution of carbon composite sample SG1 (left) and SG3 (right).....	30
Figure 28 Pore size distribution of carbon composite sample SG4	31
Figure 29 SEM images of the SG1 sample (HPC with nickel)	31
Figure 30 SEM images of the SG4 sample (HPC without salt)	32
Figure 31 The X-ray diffraction patterns of carbon composite with HPC/NiCl ₂	32
Figure 32 Low temperature nitrogen sorption isotherms of carbon sample SG5 (left) and SG8 (right)	33

Figure 33 Low temperature nitrogen sorption isotherms of carbon sample SG9 (orange) and SG10 (black)	33
Figure 34 Low temperature nitrogen sorption isotherms of carbon sample SG11 and SG12	34
Figure 35 Low temperature nitrogen sorption isotherms of carbon sample SG13 (left) and SG14 (right)	34
Figure 36 Low temperature nitrogen sorption isotherms of carbon sample SG15 (left) and SG16 (right)	34
Figure 37 Low temperature nitrogen sorption isotherms of carbon sample SG17 and SG18	35
Figure 38 Pore size distribution of carbon composite sample SG17 and SG18	36
Figure 39 Pore size distribution of carbon composite sample SG11, SG12 and SG8	37
Figure 40 SEM images of the sample SG11 (left) and SG12 (right).	37
Figure 41 SEM images of the SG11 (left) and SG12 (right)	38
Figure 42 SEM images of the sample SG16 monolith and SG16 powder	38
Figure 43 SEM images of the of sample SG17	39
Figure 44 SEM images of the of sample SG18	40
Figure 45 X-ray diffraction patterns of carbon material: CA/CoBr ₂ samples	40
Figure 46 X-ray diffraction patterns of carbon material: CA/CoCl ₂ sample	41
Figure 47 X-ray diffraction patterns of carbon material: CA/Co(NO ₃) ₂ samples	41
Figure A1 Timeline	52

List of Tables

Table 1 Textural characteristics of C/SiO₂ samples synthesized from HPC containing xerogels	30
Table 2 Textural characteristics of carbonized CA containing xerogels.....	35
Table A1 composition of precursor/SiO₂ samples	49
Table A2 Time required to form gels in the presence of HPC.....	50
Table A3 Characteristics of gels prepared in the presence of CA	50
Table A4 Comparison of acid and basic catalyst protocol	51
Table A5 Characterization methods performed in each sample	53

List of Equations

Equation 1 Hydrolysis of TEOS molecules (alkoxide precursor) in an acid catalyzed sol-gel reaction..	9
Equation 2 Condensation of TEOS molecules in an acid catalyzed sol-gel reaction.....	10
Equation 3 Condensation of TEOS molecules in an acid catalyzed sol-gel reaction.....	10
Equation 4 The thermal decomposition of Co(NO ₃) ₂	39

Abbreviations and symbols

BET	Brunauer, Emmett and Teller
CA	Cellulose acetate
FCC	Face-centered cubic
FTIR	Fourier transform infrared spectroscopy
hcp	hexagonal close-packed
HPC	Hydroxypropyl cellulose
IUPAC	International Union of Pure and Applied Chemistry
SEM	Scanning Electron Microscopy
SG _i	Sol-gel sample (i= 1 to 19)
TEOS	Tetraethylortosilicate
TGA	Thermo Gravimetric Analysis
XRD	X-Ray Diffraction

1 Problem Statement

Nanotechnology is the way of ingeniously controlling the building of small and large structures, with intricate properties; it is the way of the future, with incidentally, environmental benignness built in by design

Professor Hoffmann; Nobel prize in Chemistry; Cornell University

Nanomaterials have profound applications in many fields including microelectronics, manufacturing, medicine, clean energy and environment. These materials have tremendous potential in enabling process innovations in areas such as, hydrogen storage, alternative solar cells, gas to liquid conversion, fuel cells and batteries [2]. One of the biggest challenges is finding materials that could store a significant amount of energy. Nanostructured carbon materials are among the most promising energy storage candidates, since they have unique features, such as electrochemical capacity, tunable porosity, high surface area, large pore volume, facile functionalization and high physicochemical stability. Porous nanostructured carbon materials could be prepared in silica templates through sol-gel technique followed by carbonization of carbon precursor [3].

1.1 Description of Project work plan

This master thesis of Chemical Engineering degree was conducted at the department of Microtechnology and Nanoscience, at Chalmers. The objectives of this thesis can be summarized under the following four items:

1. Review of existing literature on the sol-gel approach for the synthesis of carbon/silica nanocomposites;
2. Synthesis of cellulose derivative/silica gels containing Ni(II) and Co(II) salts by sol-gel technique;
3. Synthesis of porous Ni(Co)/C/SiO₂ composites by carbonization of cellulose derivative/silica xerogels containing Ni(II) and Co(II) salts;
4. Analysis of synthesized materials with FTIR, SEM, XRD, TGA and low temperature nitrogen sorption;

1.2 Overview of thesis

Chapter 1 explains the motivation and the work plan of this master thesis project.

In chapter 2 the concepts of nanomaterials and the challenges that cellulose nanocomposites face are described. This chapter also includes the concept of a carbon nanocomposite material containing transition metals, a description of sol-gel process and the literature review.

The aim of this project is described in chapter 3.

Chapter 4 presents methods and materials used in the synthesis of porous Ni(Co)/C/SiO₂ nanocomposites. The chapter covers the development of all stages of production required for the manufacture of the desired material. Chapter 4 reviews also the testing that the novel materials were subjected to for purposes of identifying their structure and physical characteristics.

Chapter 5 reviews the results obtained in this work and their discussion.

2 Background of the study

2.1 Porous carbon nanomaterials

Carbon is a very important element for all living things on the Earth, including humans, because all organic compounds are composed from carbon networks

Michio Inagaki, *New Carbons: Structure and Texture of Carbon materials*, Elsevier Science, p. 1(2000)

Carbon nanomaterials represent a revolution in science and many of the current and future technological challenges have as a solution the use of carbon nanomaterials because of their promising electrical, mechanical, chemical and optical properties [2]. Carbon nanoporous materials with controlled morphology and surface properties are prospective for functional applications such as gas storage, catalysis, chromatography, separation, and sensing [2, 3]. They are inert, chemically, mechanically and thermally stable [2].

There are two kinds of pores in carbon materials: closed pores and open pores. Materials with closed pores are useful in thermal insulation or as lightweight materials for structural applications. Open pores, are connected with material surface and are used for separation, catalysis and sensing applications [2]. Porous materials can be classified by size, network forming material and degree of order. According to International Union of Pure and Applied Chemistry (IUPAC) definition, the material is microporous if the pores are smaller than 2 nm, mesoporous if they are up to 50 nm and macroporous if the pores are over 50nm [4].

2.1.1 Methods for the synthesis of porous carbon materials

Nanoporous materials can be synthesized by various methods such as template route, liquid crystal, self-assembling, supercritical extraction and swelling (Figure 1) [5].

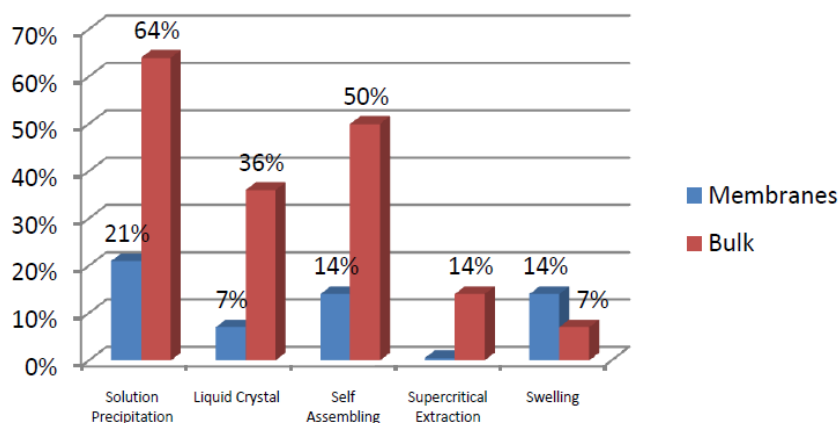


Figure 1 Typical methods used for the synthesis of nanoporous materials [5]

Liquid crystal route could lead to large continuous domains of mesoporous structures. This method has some disadvantages like price and technical obstacles and the need for new templates also involves expensive synthetic procedures [5].

Self-assembling process involves designing atoms and molecules so that shape-complementarily causes them to aggregate into desired structures [6]. Self-assembly has a number of advantages because this process is a bottom-up approach and does not require scaling down the manufacturing tools presently required. This method requires a smaller amount of raw materials and produces less waste [5].

The supercritical extraction process is used to produce well-defined nanostructures for potential applications in inorganic catalyst supports [5]. This method is the process of to separate the extractant from the matrix using supercritical fluids as the extracting solvent. Carbon dioxide is the most used supercritical fluid and this process is very good to control solvent variables. The lower viscosity of supercritical fluids allows an easier penetration into the porous structure, but there are questions like price and technical barriers that need to be overcome [5].

The swelling process involves the absorption of a solvent with the increase of volume of material. The swelling behaviour of polymer cross-linked matrices depends on the degree of cross-linking of the blocks. This process allows the control of the internal surface characteristics of the nanoporous materials since the presence of double bonds in the nanoporous polymer facilitates a controlled introduction of functional groups onto the pore walls [5].

The template synthesis method can be used to produce materials of carbon with unusual properties [3, 7]. This method leaves an ordered framework is a new trend in carbon research [7]. It is one of the most important techniques and has been of interest to many researchers for the reason that it has proven to be a feasible method for the preparation of well-structured porous carbons with pore sizes that span from micropores, mesopores and macropores [8]. The template synthesis method also has the unique advantage of being easy, inexpensive and can be properly adapted for large-scale production [7].

According to nanoroadmap [5], sol-gel techniques became much demanded since this route is a versatile method allowing producing bulk materials, either crystalline or amorphous of controlled porosity, as well as fibers, films and nanoparticles. This process is a good method to control the morphology of pores in carbon nanomaterials since this process allows a good control of the textural characteristics of the material, and a better dispersion of cobalt/nickel salts into the silica matrix [9]. Sol gel assisted way could be good for the synthesis of carbon materials as well.

2.1.2 Applications of carbon porous materials

Porous carbon materials are important in many areas of modern science and technology, including energy storage, water and air purification, gas separation and catalysis [2].

High surface area of porous nanomaterials can be used in the clean energy production and storage. Future energy supply is dependent on clean energy such as hydrogen energy. In the future, hydrogen can be the dominant fuel to convert electricity in fuel cells [10]. In this way, certain nanoporous materials have already shown to be promising for application in fuel cells as an adsorbent and electrodes [2]. For applications in energy storage is necessary to have highly porous materials with high specific surface area and incorporation of transition metals in the material [11].

Carbon mesoporous materials templated with silica exhibit interesting performance as supercapacitor and electrode materials for battery applications [12]. Creating a material with higher surface area, storage devices can hold more charge. These materials can be used in ultracapacitors as electrodes, as it can be seen in Figure 2-3. Ultracapacitors, which charge and discharge power quickly, are being considered as a complement to batteries for some applications, including electric vehicles [1].

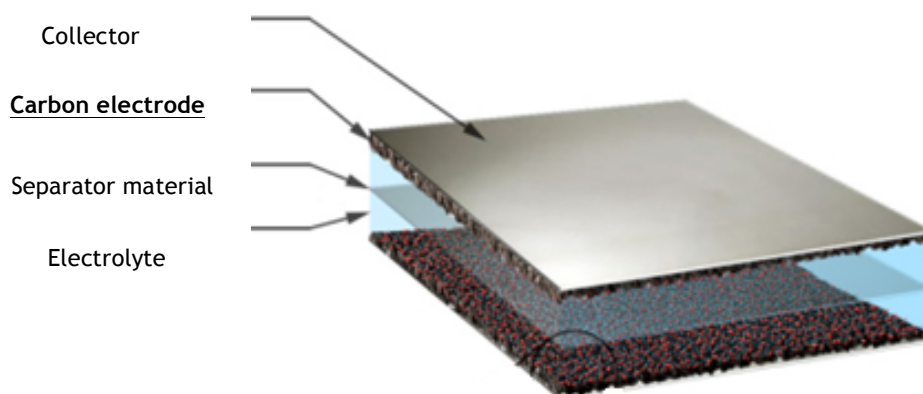


Figure 2 Carbon electrode for battery applications [1]

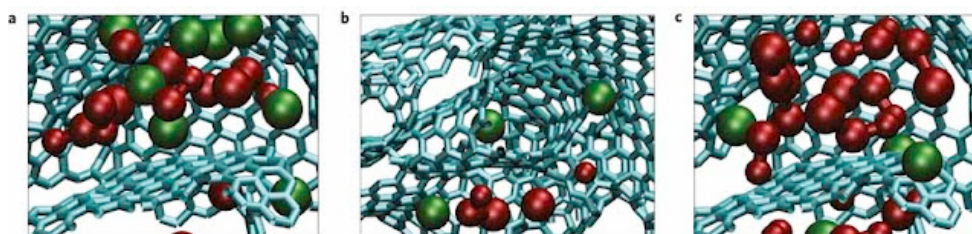


Figure 3 'On the molecular origin of supercapacitance in nanoporous carbon electrodes'[13]

Lithium ion batteries are among the best-performing batteries because of their combination of relatively high power and energy density. These batteries (Figure 4) use a lithium-based oxide cathode, which can store a large quantity of lithium but is not conductive. In order to improve the conductivity of carbon to the cathode reduces resistance and increases the power capability of the cell [1]. The graphite anode will be replaced with high surface area carbons and lithium-alloying elements such as silicon, aluminium which will enable doubling or tripling energy and power density. This could result in longer-lived batteries with more power and energy for all kinds of applications, including consumer electronics such as laptops and cell phones, as well as hybrid or plug-in vehicles [1, 14].

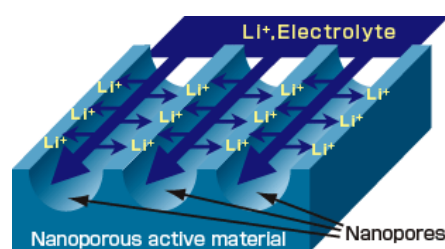


Figure 4 Diffusion path of lithium ions (Li+) through nanopores of a nanoporous active material [14].

Carbon nanoporous materials offer possibilities for catalysis because of their controlled large and accessible surface area. The impregnation of transition metal impart wide range of physical, chemical and optical properties that can have impact on chemical production, environmental protection, processing of consumer products and advanced materials [2]. As nanoscale catalysts becomes mainstream and moves into more established industries low-cost nanostructured carbon to be a key support material for improving the efficiency of the reactions ranging from pharmacy and food to bulk chemicals energy [1].

Carbon nanoporous materials can be used for sensors materials since these materials possess large specific surface area and high sensitivity to slight changes in temperature, humidity and light [2].

2.2 Silica is promising template for the synthesis of carbon porous nanomaterials

Silica is the most available compound in the world [15]. Amorphous silica is largely used in industrial applications, mainly in the amorphous form because of its properties like high hardness, thermal and chemical stability. An important characteristic of amorphous silica is the possibility to be arranged in various complex structures such as monoliths, nanoscale particles and porous silica [16].

SiO₂/carbon xerogels can be prepared by sol-gel polycondensation of TEOS and carbon precursor, followed by drying and carbonization [17]. Carbon increases the surface area and hydrophobicity of the carbon-silica gel composites [18]. The pore structure of xerogels composites is formed mainly by carbon. The SiO₂/carbon xerogels could be synthesized with excellent characteristics, such as high surface area, high porosity, controlled pore size, high density and high conductivity and may be prepared in monolith form [3, 18].

One of the most characteristic features of sol-gel derived silica xerogel is an amorphous pore structure. The reactivity of the matrix, due to free hydroxyl groups, is the other typical property of silica xerogel [15, 16].

The porous texture and chemical structure of the SiO₂/carbon xerogels can be customized at the specific needs of the process that will be used. The porous texture of these carbon xerogels depends on the variables of synthesis: the type of precursor, the pH of the sol-gel process, process of gel drying and carbonization. In low pH situations, the silica particles can

collide and aggregate into chains and then form gel networks because these particles bear very little ionic charge [3, 18]. When the gel is dried, xerogels are obtained. Evaporation may be carried out in ambient conditions or at elevated temperatures, in natural or forced convection. During the drying process, the material has a tendency to shrink due to the capillary forces and material obtained after the carbonization is sometimes non-porous. However, by controlling synthesis variables, materials with well developed porous structure can be produced [16].

2.3 Sol gel process

The nanostructured C/SiO₂ composites can be obtained from the carbonization of silica composites containing organic precursor. Sol-gel technology is often used in the synthesis of nanoporous materials and in this technique the gel is formed from hydrolysis and condensation of a precursor of structure forming agents. Amorphous materials in various forms, including coatings, powders, fibers, films, monoliths and porous membranes could be produced by this process [19]. The sol-gel process involves the formation of a colloidal suspension (sol) and the gelation of the sol resulting in the formation of tridimensional network-gel, which after drying forms a xerogel [16].

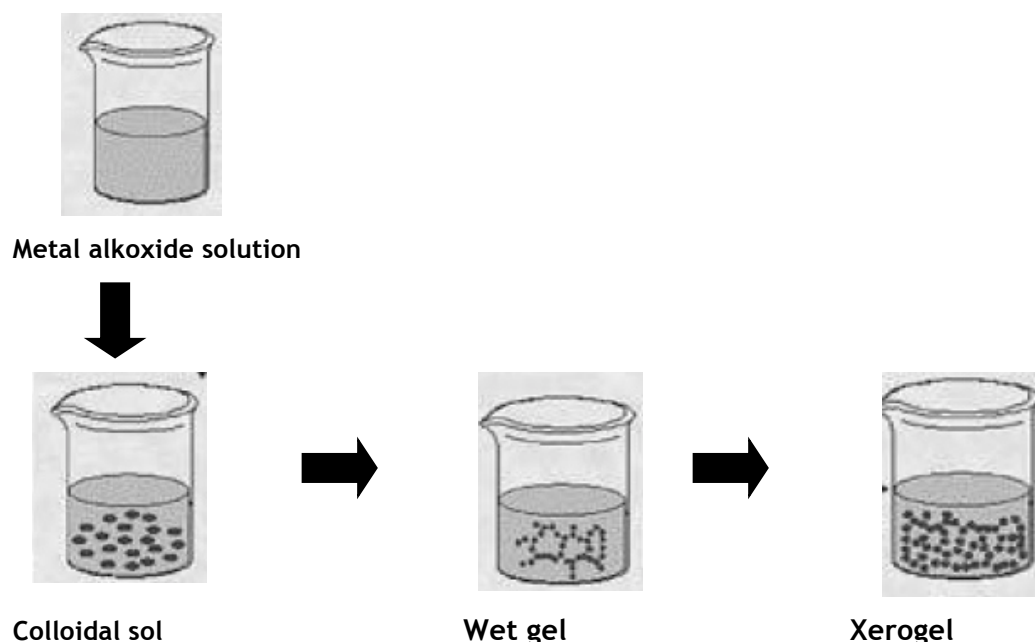


Figure 5 Steps of the sol gel process

Main steps of the process are hydrolysis and condensation reactions followed of gelation, ageing and drying (Figure 5) [19].

2.3.1 Formation of silica sol by hydrolysis of TEOS

The sol gel process begins with the preparation of an initial solution containing the precursor, dispersion medium, water, in the presence of acid or basic catalyst. Tetraethoxysilane (TEOS) is the most widely used alkoxide precursor for a sol-gel reaction. This precursor is immiscible in water (Figure 6) and then is necessary to use an alcoholic solvent, which acts as a homogenizing agent [16].

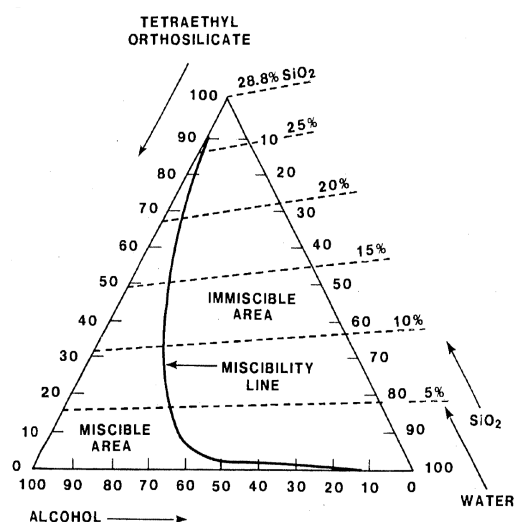
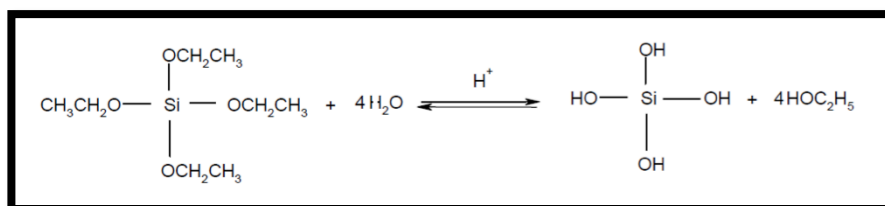


Figure 6 TEOS, H₂O and alcohol ternary phase diagram. For pure ethanol the miscibility line is shifted slightly to the right [16].

The first step in sol-gel process is hydrolysis of TEOS resulting in formation of silanol groups (Si-OH) and ethanol as shown in Equation 1. The reaction occurs by the nucleophilic attack of oxygen on the silicon atom and can occur in presence of a base or an acid [16, 19].

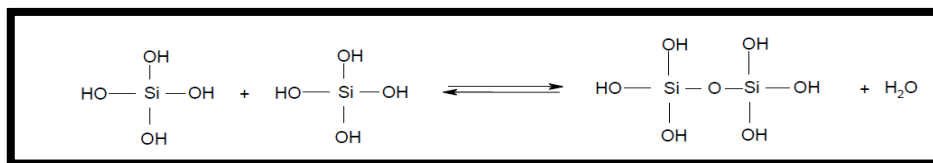
The kinetics of the hydrolysis reaction is slow and occurs simultaneously with the condensation processes [16].



Equation 1 Hydrolysis of TEOS molecules (alkoxide precursor) in an acid catalyzed sol-gel reaction.

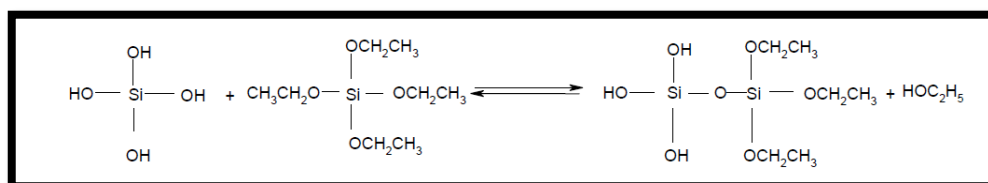
During condensation reactions between silanol groups siloxane bonds (Si-O-Si) are formed (Equation 2-3).

Condensation



Equation 2 Condensation of TEOS molecules in an acid catalyzed sol-gel reaction.

The condensation reactions release water and ethanol (Equation 2-3) into the solution as the SiO₂ matrix forms (Figure 7). Condensation and polymerization leads to the growth of particles that depends on various conditions such as pH [16].



Equation 3 Condensation of TEOS molecules in an acid catalyzed sol-gel reaction.

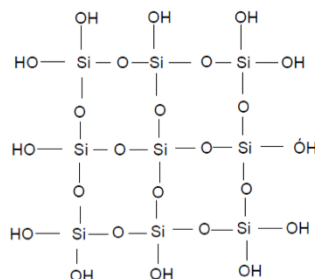


Figure 7 Silica matrix

Process of the gel formation consists of two steps. In the first step, with increasing the concentration of polymerizable species formed during the hydrolysis and condensation, the probability of forming a polymer network leading to gelation also increases [15]. At the second step when the number of connections between these species is sufficient for the formation of a three-dimensional structure, a sol-gel transition (gel point) occurs [16].

2.3.2 Gelation

During gelation, a tri-dimensional network that binds the whole remaining solution is formed. In this step the gel has a high viscosity and the chemical composition of the mixture could be affected [19, 20].

2.3.3 Ageing

During ageing, additional cross-links form. Covalent links replace nonbonded contacts. Shrinkage of gel occurs during this step, the ripening and structural evolution of pore sizes and pore wall strengthening occurs [20].

2.3.4 Drying

Drying the gel is the loss of the dispersion medium by evaporation. It results in a porous xerogel. Structure of xerogels is affected by drying conditions. Drying by evaporation under normal conditions gives rise to capillary pressure that causes shrinkage of the gel network resulting in xerogels [16, 20]. During this drying process the material has a tendency to shrink due to the capillary forces that are established in the pores.

2.3.5 Factors affecting the sol-gel process

By controlling the hydrolysis and gelation conditions, is it possible to produce materials with well developed porosity.

i) Effect of Water-to-alkoxide molar ratio

The water/alkoxide molar ratio has considerable effect on the silica xerogel microstructure [16]. The formation of more microporous materials occurs when the water/alkoxide molar ratio is low, since condensation reactions are dominating and gelation time is longer. Gels made from higher water content sol (water/alkoxide molar ratio up 4) have shown less microstructure than gels made from lower water content sols [21]. The gels synthesized from lower water content have more unreacted alkoxy ligands than those from higher water content sol and therefore form more linear chain-like structures and more split polymers are formed [16].

ii) pH effect

The effect of pH on the pore structure of the xerogels and morphology has been extensively studied [16]. The kinetics and growth mechanisms of the reaction depend on the pH value of solution. The relative rates of hydrolysis and condensation effectively determine the morphology of the final xerogel [15]. The gelation times reach a maximum around pH ~2, which coincides with the point-of-zero-charge (PZC) of silica (Figure 8).

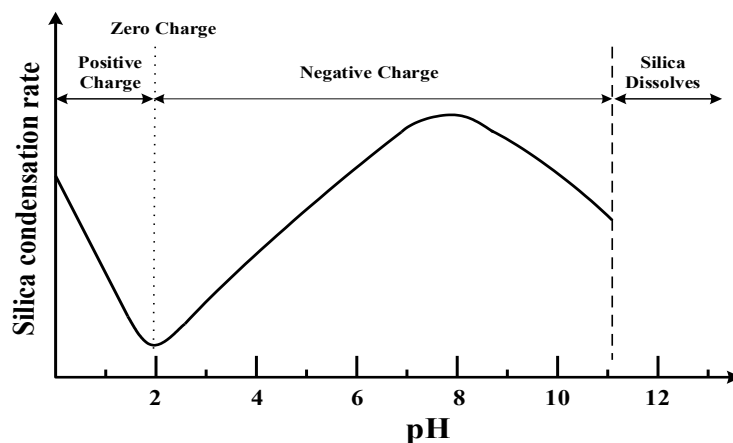


Figure 8 Point-of-zero-charge (PZC) of silica [15].

At moderate pH, condensation is fast relative to hydrolysis, which results in the formation of highly branched silica species. They form loosely packed, cluster-like structures that coalesce leaving mesoporous regions between them. As the pH decreases and approaches the PZC (pH ~2) condensation becomes rate limiting (the condensation rate is the slowest) [16].

In the region of very low pH (<1), below the PZC, the trend in gelation time dramatically reverses and sols form gel quite rapidly. This is attributed to an increased rate of condensation due to the protonation of silanols to produce SiOH₂⁺ groups that readily condense [15, 16]. Based on these kinetic arguments, it would be anticipated that the decreasing gelation times at very low pH would be accompanied by an increase in porosity [16, 20].

2.4 Cellulose: fascinating biopolymer

Cellulose is the world's most abundant natural, renewable and biodegradable polymer

Azizi Samir, M.A.S.; Alloin, F.; Dufresne, *Biomacromolecules*, 6, 612-626 (2005).

The depletion of petroleum resources and more rigorous environmental issues led to considerable research efforts on development of biopolymeric materials. The advantage of using cellulose derivate materials is that, unlike fossil fuels, they cannot become exhaust because they can be cultivated in required quantity as and when needed [22].

The synthesis of environmentally friendly materials is a challenging task and can be developed by modifying inexpensive natural renewable resources.

The combination of cellulose and sol-gel science could be of high interest. Cellulose/silica composites are of especial interest because improved thermal and mechanical stability of the parent polymer matrix [23, 24]. Cellulose/silica materials could be highly porous and light weighted, yet mechanically stable, and could possess complex pore structure.

The drawback of cellulose is that it is insoluble in most solvents, which significantly decreases its potential for preparation of functional materials. Cellulose derivatives are soluble in a wide range of solvents, which makes them to be prospective for production of various composites [22].

2.4.1 Cellulose acetate

Cellulose acetate is a thermoplastic polymer produced primarily from cellulose, a renewable feedstock (Figure 9) [25]. Cellulose acetate has applications in many areas such as supports for fibers, plastics, photographic film, and coatings for pharmaceuticals. Some limitations can be identified, including poor resistance to mechanical creep, and limited resistance to organic solvents. This cellulose derivative is soluble in acetone or water/acetone mixture [26].

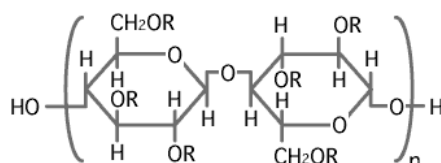


Figure 9 Chemical structure of cellulose acetate

2.4.2 Hydroxypropyl cellulose

Hydroxypropyl cellulose (HPC) is a biopolymer obtained from the chemical modification of cellulose (Figure 10). Although it is hydrophobically modified, it has quite high solubility in water. HPC undergoes phase separation upon heating, and it is able to form liquid crystals [27]. This polymer has been used in the consolidation of waterlogged woods and it was revealed very efficient even if optimization of the impregnation process was necessary [24]. HPC ensures the stabilization and the homogeneity of the dispersion of inorganic salts, and therefore, is used in the preparation of organic-inorganic nanocomposites [28].

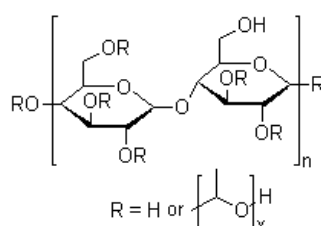


Figure 10 chemical structure of hydroxypropyl cellulose

There are a few studies about the preparation of hybrid materials based on cellulose derivatives, particularly hydroxypropyl cellulose [24, 28] and cellulose acetate [25, 26]. In 1994 Schoirchiro Yano prepared materials about hydroxypropyl cellulose (HPC)/silica although sol-gel method, from TEOS. They used 5 wt% ethyl alcohol solution of HPC, which is concentrated enough to form liquid crystal [24].

Shojaie et al. (1995) prepared and characterized a series of hybrids films with cellulose acetate and silica through sol-gel method using TEOS as chemical precursor [25].

In 2002, Zoppi and Goncalves studied the formation of membranes with cellulose acetate [26].

2.4.3 Carbonization of cellulose

The objective of the carbonization step is to obtain thermally stable materials, mostly composed of carbon atoms. These carbon nanostructured materials are usually obtained by carbonization of the organic precursor. Usually, gels are carbonized by heating the samples in a furnace under inert atmosphere (N₂, Ar or He) for a specific period of time [29]. The temperatures may vary depending on the nature of the precursor. It is well known that cellulose is very cheap and user friendly during pyrolysis due to production of nontoxic products [22, 30]. During the carbonization process, cellulose is decomposed into carbon substance. Cellulose is unique among biopolymers in that when it is charred below 400°C and above its decomposition temperature of 280 °C it produces an aromatic structure in which

domains of aromatic hydrocarbon. This process involves the loss of water up to about 120°C, and after that the dehydration process takes place up to 300°C resulting in dehydrocellulose. At the same time depolymerisation occurs at 250°C forming levoglucosan [30]. The products of this process include highly volatile gases, as can be seen in the picture below (Figure 11).

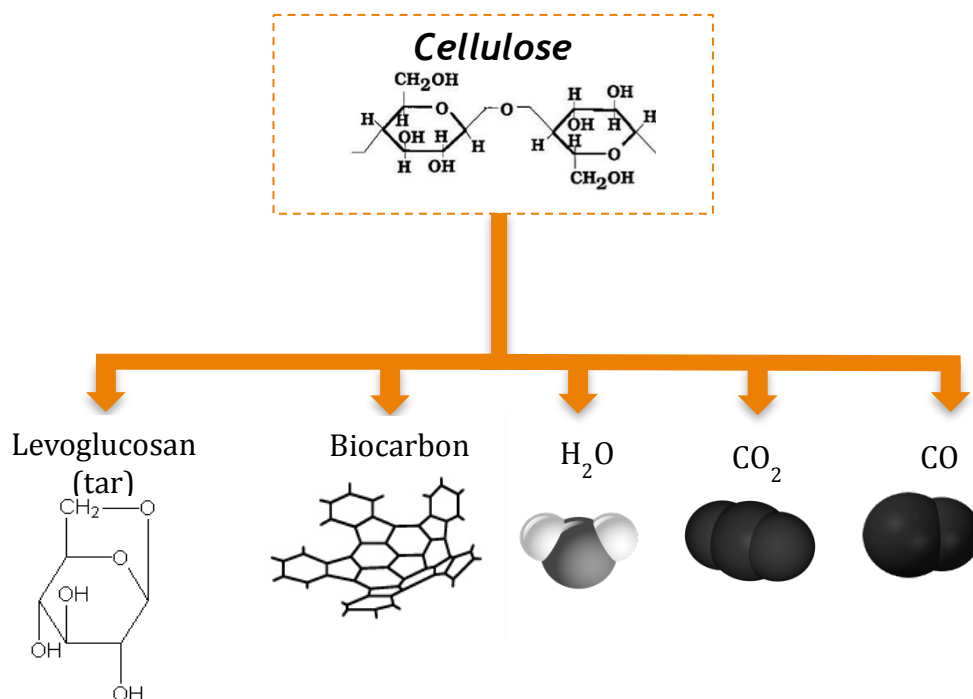


Figure 11 Scheme of cellulose decomposition during carbonization

2.5 Modification of properties of carbon materials with transitional metals

The presence of a transitional metal in the structure of carbon nanomaterial can improve the electrical conductivity of the xerogel, and gives the xerogel some catalytic properties characteristic to the metal [29]. These metals salts are used in order to enhance hydrogen adsorption on carbon nanomaterials since the incorporation of these metals into the porous carbon framework is due to the fact that these metals should modify the electrical properties of carbon materials. Such materials with metal salts can be easily prepared by adding a soluble metal salt to the initial mixture. The morphology and pore texture of the xerogel can be affected by the addition of these metals since the metals can catalyze the polymerization or gelation process to a varying degree. During gelation, the metal salt is trapped within the structure of the gel, and during carbonization the metal is distributed through the porosity of

the carbon [31, 32]. The nanoporous carbons with incorporated transitional metals have high electroconductivity and high surface areas. They are promising for a large range of potential applications, such as hydrogen storage [33], electronic devices and catalysts.

2.5.1 Cobalt

Co is a well-known ferromagnetic material, which is commonly used as an alloying element in permanent magnets. It exists in two forms: hcp (hexagonal close-packed) and fcc (face-centered cubic). Hcp is the stable phase at room temperature, whereas fcc is stable at temperatures above 450 °C [34].

In nanosize, Co particles display a wide range of interesting size-dependent structural, electrical, magnetic, and catalytic properties [35]. In particular, because of their large surface area, Co nanoparticles showed high chemical reactivity, which makes them suitable for catalysis [36].

2.5.2 Nickel

Natural nickel corresponds to a mixture of stable isotopes and its main ferromagnetic behavior is enhanced above 358°C and reacts slowly with strong acids [37]. Nickel is crystallized in two forms: hexagonal and cubic. Nickel forms a large amount of complex compounds in which it shows various oxidation states. The oxidation state +2 is the most common.

Soo-Jin Park et al. investigated the hydrogen-storage capacity of mesoporous MCM-41 containing nickel (Ni) oxides. This work shows that the hydrogen storage capacity was greatly influenced by the amount of nickel oxide creating hydrogen favorable sites that enhance the hydrogen-storage capacity by a spillover effect [38].

3 Aim of the work

The aim of this research project was the synthesis of Ni(Co)/C/SiO₂ composites by the sol-gel approach from cellulose derivatives and TEOS in the presence of Ni(II) and Co(II) salts. These polymers were chosen as carbon precursors because of their renewability and low cost.

Ni(Co)/C/SiO₂ composites synthesized in this work were investigated with low temperature nitrogen sorption, powder X-ray diffraction, scanning electron microscopy and thermal gravimetric analysis .

4 Materials and Methods

4.1 Synthesis of silica xerogels

4.1.1 Materials

Tetraethylorthosilicate (TEOS, 98%, Aldrich), Cellulose acetate (CA, Mn~30.000, Aldrich), hydroxypropyl cellulose (HPC, Aldrich), acetone (99.9%, Solveco), ethanol (95% Solveco), cobalt chloride hexahydrate (ACS grade, Alfa Aesar), cobalt bromide anhydrous (ACS grade, Alfa Aesar), cobalt nitrate tetrahydrate (ACS grade, Alfa Aesar), nickel chloride hexahydrate (ACS grade, Alfa Aesar), and hydrochloric acid (HCl, 99%, Solveco) were used as purchased without any purification.

4.1.2 Preparation of cellulose solutions

CA solution (C=3g/100mL) was prepared in volumetric flask at room temperature. HPC solution (3g/100mL) was prepared from 3g of HPC and 100 mL of ethanol at room temperature. Prepared solution was kept in tightly closed flasks in shaker overnight prior to use.

4.1.3 Preparation of metal salts solutions

0.42M solutions of CoCl₂, NiCl₂, Co(NO₃)₂, CoBr₂ in water were prepared from CoCl₂.6H₂O, NiCl₂.6H₂O, Co(NO₃)₂.4H₂O, CoBr₂ anhydrous.

After preparation, the solutions were kept in tightly closed flasks in dark place for 24h prior to use.

4.1.4 Sol-Gel Process

i) Sol-gel Reactions

The synthesis of the silica nanostructures through sol-gel approach consisted in the addition to the solution of carbon precursor (cellulose acetate or hydroxypropyl cellulose), silica

source - TEOS, and Ni(II) or Co(II) salt solution. A catalyst, hydrochloric acid was added in order to activate the sol-gel process and to accelerate hydrolysis and condensation reaction of TEOS. The resulting mixture was heat at 50 °C for a 1 or 5 hours with vigorous stirring. Control samples were also prepared under similar conditions using deionized water instead of Ni(II) or Co(II) salt solution.

Composition of prepared samples is presented in Appendix (Table A1).

ii) Ageing

The prepared precursor/SiO₂ solutions were transferred into plastic containers and put to ageing at 45 °C in oven for 5 and 90 days.

iii) Drying

Gels were dried at room temperature under fume hood. In case of syneresis excess of liquid was removed from gel by syringe prior to drying.

4.2 Synthesis of carbon nanocomposites

Carbonization was performed at 800 °C with 5 °C/min of heating ramp, under an inert atmosphere of nitrogen with flow of gas around 1L/min. Samples were placed into the tube furnace (Figure 12a) in alumina crucibles (Figure 12b). After 2 hours of keeping samples at 800 °C, the heating was stopped and samples were left in oven until the temperature inside reached room temperature.

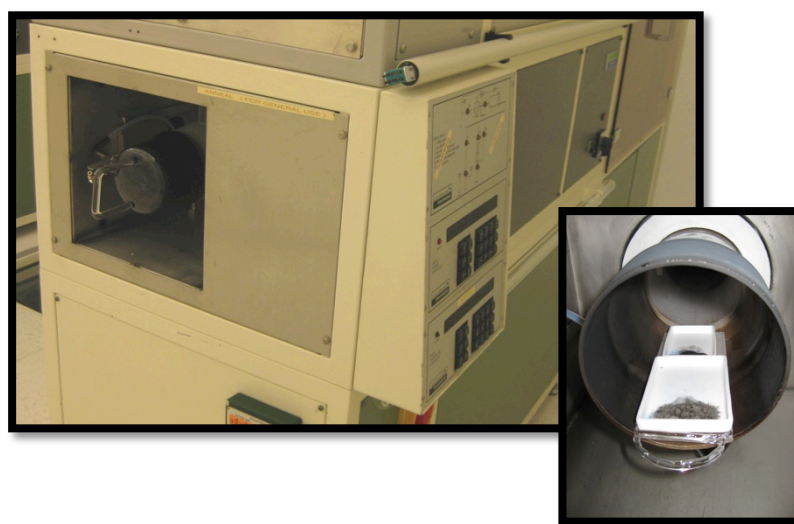


Figure 12 a) The furnace in cleanroom b) powder samples in alumina crucibles after carbonization

4.3 Characterization techniques

This section describes the characterization techniques and the evaluation procedures used to analyze the synthesized nanomaterials. These characterization methods of the synthesized materials include: N₂ adsorption, Scanning Electron Microscopy (SEM), Thermo Gravimetric Analysis (TGA), X-ray Diffraction (XRD) and Fourier transform infrared spectroscopy (FTIR). More details about the methods applied for the characterization performed in each sample can be found in Appendix (Table A5).

4.3.1 Specific surface area

The specific surface area can be estimated on the basis of the N₂ volume adsorbed on the material's surface [39] at an isothermal temperature of 77 K as a function of the N₂ relative pressure (P/P_0). In this work, the classical model to determine the specific surface area from the nitrogen volume adsorbed on the material's surface developed by Brunauer, Emmett and Teller [40] has been used.

The determination of specific surface by means of the BET theory is based on the phenomenon of physical adsorption of gases on the external and internal surfaces of a porous material. This material absorbs physically a certain amount of gas that surrounds it at a certain temperature, T and relative vapour pressure p/p_0 . The relationship between relative vapour pressure and amount of adsorbed gas at a constant temperature is called an adsorption isotherm. The amount of gas adsorbed depends on the size of the pores within the sample and on the partial pressure of the gas relative to its saturation pressure. By measuring the volume of gas adsorbed at a particular partial pressure, the BET equation gives the specific surface area of the material. The Kelvin equation gives the pore size distribution of the sample in hysteresis at high partial pressures from adsorption/desorption curves [39].

Nitrogen sorption isotherms were recorded with Tristar 3000 (Micromeritics) at -196°C.

From low temperature N₂ adsorption-desorption isotherms one can receive information about the morphology of porous material, as specific surface area, micropore volume and diameter of mesopores.

4.3.2 Thermo gravimetric analysis (TGA)

The thermo-gravimetric analysis determines the loss of organic matter with temperature. These analyses were performed on a Pyris TGA 7 (Perkin Elmer) equipment. The range of

temperatures measured was until 800°C at heating rate to 5°C/min under nitrogen atmosphere.

Thermal analysis provides an explanation of behavior of the carbonization process. In results from TGA is possible to see the weight loss in percentage with temperature increase, which represent the decomposition of organic groups of the xerogel.

4.3.3 Scanning Electron Microscopy (SEM)

Scanning electron microscopy is an indispensable tool for the investigation of porous materials. This microscopy method is a type of electron microscope that images are produced out of interaction of the electrons with the atoms on the sample surface. In this project samples were studied with Zeiss Leo Ultra 55 FEG SEM.

4.3.4 X-ray Diffraction (XRD)

X-ray diffraction is one of the corner stones of twentieth century science [41]. It has been widely used to characterize sol-gel nanoporous materials. Crystalline structure of the synthesized material was examined by XRD method (Philips X'Pert Materials Research Diffractometer (MRD)). Radiation was generated with an X-Ray tube with a Cu anode ($K\alpha$ radiation, $\lambda=1.54184 \text{ \AA}$) at 45 kV and 40 mA. An X-ray lens with Ni filter was used as incident optics; a thin film collimator was used as diffracted optics. The 2θ range was $20-80^\circ$, and the resolution was 0.05° with 30s averaging time per step. Phase analysis was executed with X'Pert HighScore 3.0 (PANalytical BV) using ICDD databases (release 2008/2009).

4.3.5 Fourier transform infrared spectroscopy (FTIR)

FTIR spectra of precursor-containing xerogels were recorded with a Perkin Elmer System 2000 FT-IR spectrometer in the $4000-370 \text{ cm}^{-1}$ range with 4 cm^{-1} resolution (transmission mode) and 20 number of scans. Spectra were obtained by making pellets of 100 mg weight with ratio KBr/sample = 200/1.

5 Results and discussion

5.1 Formation of precursor containing gels

After preparation, all precursor/SiO₂ sols were transparent. No precipitation of components (even for sols with Co(II) and Ni(II) sols) was noticed. Solutions that were not aged at 45 °C did not form gels even after 3 months. Samples aged during 5-20 days usually formed gels directly in the oven.

5.1.1 Gels prepared in the presence of HPC

Solutions prepared in the presence of HPC formed gels during 6-7 days in oven. More details can be found in Appendix (Table A2). All gels were transparent and did not demonstrate syneresis (Figure 13). Xerogels remain transparent despite considerable shrinkage.

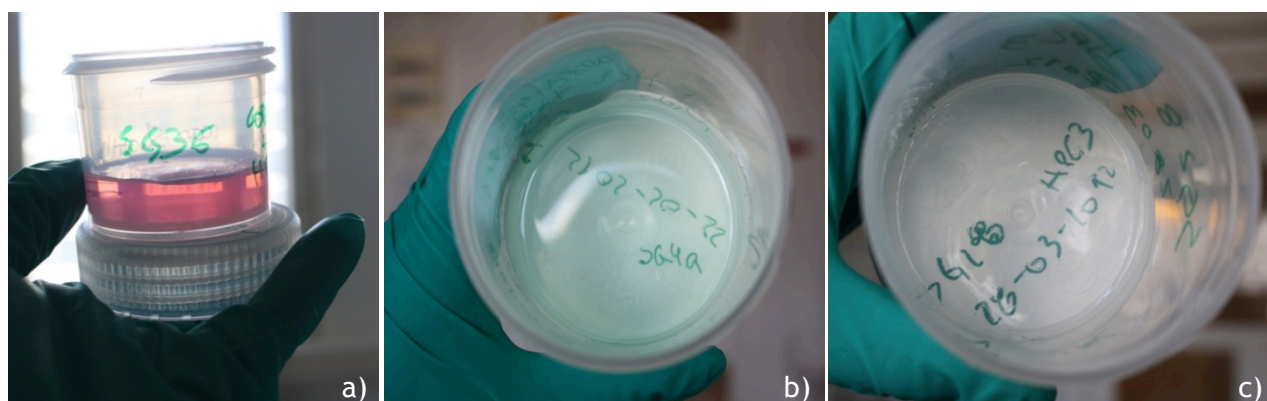


Figure 13 Gels formed in the presence of HPC - a: cobalt chloride, b: nickel chloride; c: without salt

i) Fourier transform infrared spectroscopy of carbon samples synthesized from HPC containing gels

HPC contains hydroxyl groups and then was expect it to have hydrogen bonding with the silica networks. The FTIR spectrum of HPC (Figure 14) shows a broad peak at 3440 cm⁻¹ and at 1300-1400 assigned to the O-H stretching vibration. The bands detected at 2960 cm⁻¹ and 2870 cm⁻¹ are assigned to C-H asymmetric stretching vibration of the methyl group characteristic for the hydroxypropyl group [42]. While the band at 1650 cm⁻¹ was ascribed to adsorbed water.

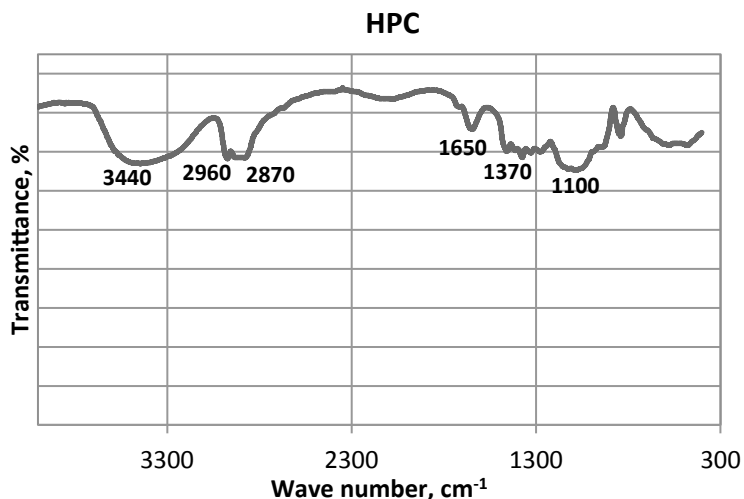


Figure 14 FTIR spectra for pure HPC

FTIR spectrum of HPC/SiO₂ (Figure 15) composite displays peaks bands assigned to OH (3440 cm⁻¹). Intensity of bands assigned to the presence of HPC/SiO₂ is decreased comparing to spectrum of pure HPC most probably due to low concentration of HPC in composites. FTIR spectrum of CA/SiO₂ composite exhibits absorption bands at 1100 cm⁻¹ from asymmetric vibration of Si-O, asymmetric vibration of Si-OH (930 cm⁻¹), and symmetric vibration of Si-O (810 cm⁻¹) [43].

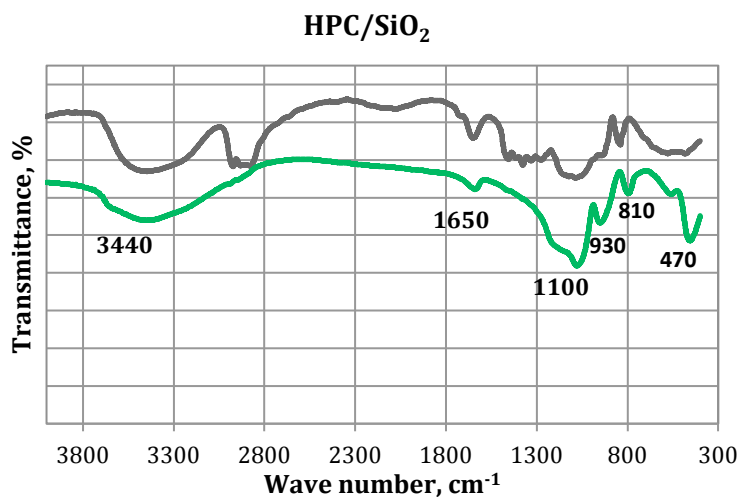


Figure 15 FTIR spectra for HPC/SiO₂ composite (green)

FTIR spectra of composites containing cobalt chloride (Figure 16) and nickel chloride (Figure 17) are very similar to HPC/SiO₂ sample. They contain bands assigned to HPC and SiO₂. No shifts in bond position were observed.

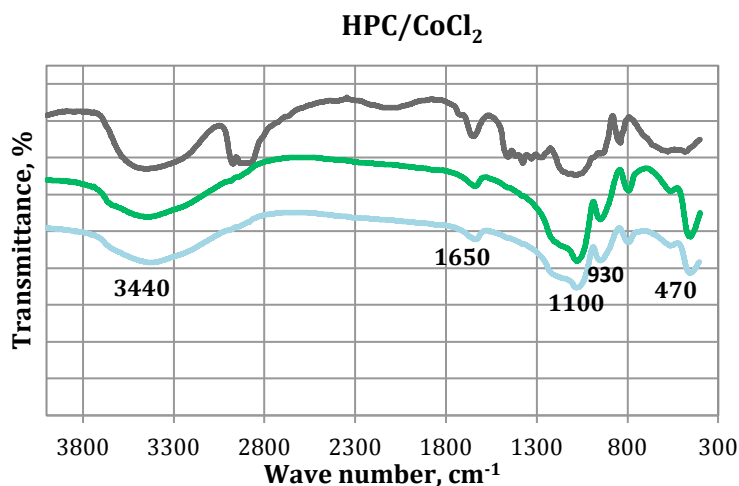


Figure 16 FTIR spectra for CoCl₂/HPC/SiO₂ (blue) composite before carbonization.

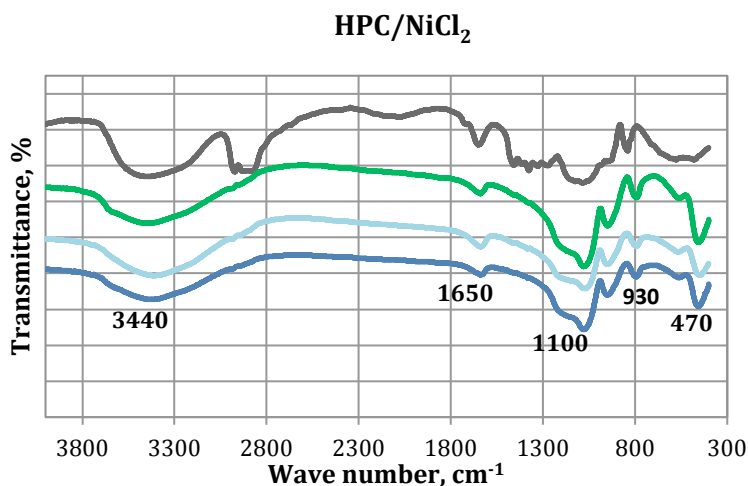


Figure 17 FTIR spectra for NiCl₂/HPC/SiO₂ (dark blue) composite before carbonization

5.1.2 Gels prepared in the presence of CA

Solutions prepared in the presence of CA formed gels during 5-26 days in oven. More details can be found in Appendix (Table A3). Gels are opaque in contrast to the transparent gels obtained from HPC solutions, as is possible to see in Figure 18. The using of cobalt bromide made it possible to prepare silica gels in five days. It is known that hydrolysis and condensation reactions affect the morphology of the gels obtained, and changing the composition of the initial solution is a good method for controlling the porosity [16].

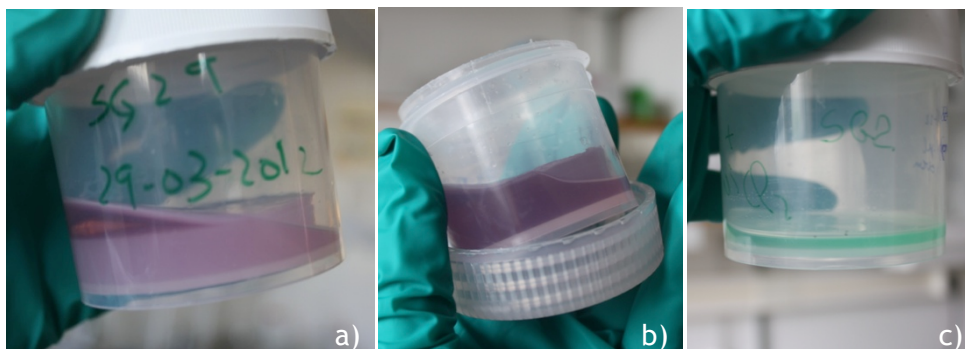


Figure 18 Gels formed in the presence of CA - a: cobalt bromide, b: cobalt bromide, c: nickel chloride.

For some samples with cobalt bromide and cobalt nitrate, the syneresis was observed after aging step (Figure 18 a), b)). Syneresis is the phenomenon of shrinkage of the gel network, which results in expulsion of liquid from the pores [19] as shown in Figure 20. Usually syneresis occurs because the formation of new bonds results from the polycondensation reaction or hydrogen bonding. It is an irreversible process in most systems of inorganic gels [16].

i) **Fourier transform infrared spectroscopy of carbon samples synthesized from CA containing gels**

The IR spectrum of cellulose acetate is dominated (Figure 19) by strong absorption band from ester group at 1760 cm⁻¹ (C=O), at 1375 cm⁻¹ (C-CH₃) for groups of the acetate substituent, 1260 cm⁻¹ (C-O-C), and band at 3540 cm⁻¹ (OH) for hydroxyl group [44, 45].

Spectrum of CA samples shows also weak bands at approximately 910 and 610 cm⁻¹, these bands are assigned to OH stretching, rocking and wagging vibrations, respectively [44].

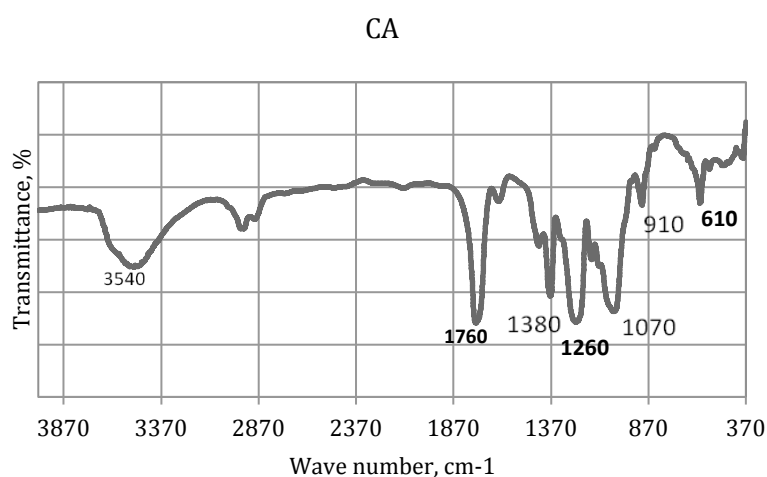


Figure 19 FTIR spectra for pure CA

FTIR spectrum of CA/SiO₂ (Figure 20) composite displays in addition to peaks assigned to the presence of CA a broadening of bands assigned to OH groups and of water (around 3500 cm⁻¹ and at 1650 cm⁻¹) due to presence of silica [46]. This spectrum shows absorption bands at 1050 cm⁻¹ from asymmetric vibration of Si-O, asymmetric vibration of Si-OH (950 cm⁻¹), and symmetric vibration of Si-O (800 cm⁻¹). There are absorption bands between 800 and 1260 cm⁻¹, which could point to various SiO₂ peaks, Si-OH bonding and peaks due to residual organic groups [43].

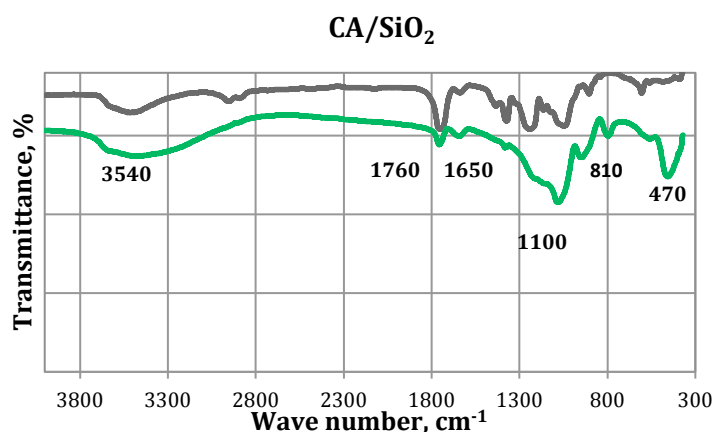


Figure 20 FTIR spectra for CA/SiO₂ composite (green)

FTIR spectra of composites containing Co(Ni) salts are characterized by further broadening of bands around 3500 cm⁻¹ and 1650 cm⁻¹ because of hygroscopicity of Co(Ni) salts and presence of coordinated water molecule [44, 47].

It is difficult to resolve bands from ester and acetate groups (1750 cm⁻¹ 1375 cm⁻¹ and 1240 cm⁻¹) in samples most probably because of their overlapping with the bands from hydroxyl groups (band at 1760 overlaps with band at 1650 cm⁻¹) and low overall concentration of CA in composite.

FTIR spectra of composites containing cobalt chloride (Figure 21) show a shift of 10 cm⁻¹ toward higher frequency for the adsorption band of ester groups (1770cm⁻¹) comparing to the FTIR spectrum of pure CA and CA/SiO₂.

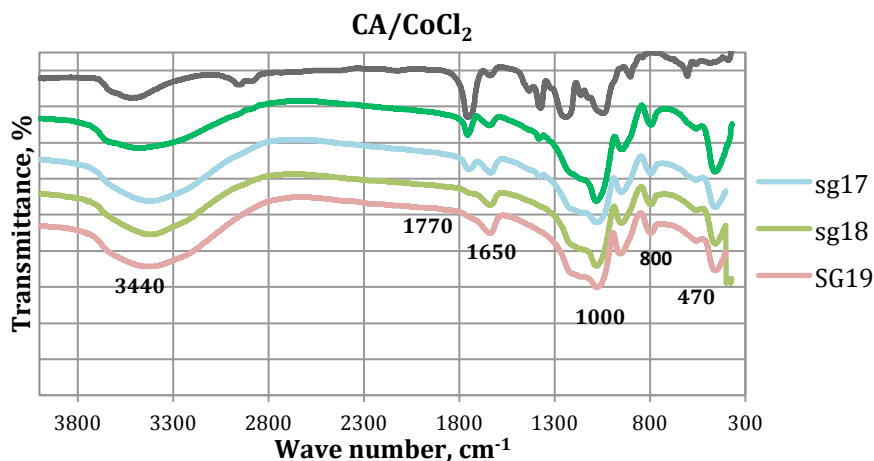


Figure 21 FTIR spectra for CoCl₂/CA/SiO₂ composite before carbonization.

FTIR spectra of composites containing cobalt bromide (Figure 22) and cobalt nitrate (Figure 23) show a shift toward lower frequency for the adsorption band of ester groups (1760cm^{-1}) comparing to the FTIR spectrum of pure CA and CA/SiO₂. The IR spectrum of samples cobalt nitrate show that the adsorption band at 1385 cm^{-1} is shifted toward higher frequency compared to the spectrum of pure CA and CA/SiO₂ composite. These shifts registered for samples with cobalt bromide and cobalt nitrate could point to complex formation between cobalt salts and cellulose acetate [47].

Formation of different complexes by Co(NO₃)₂ and CoBr₂ could explain differences in specific surface area and morphology of carbonized composites comparing to samples containing CoCl₂.

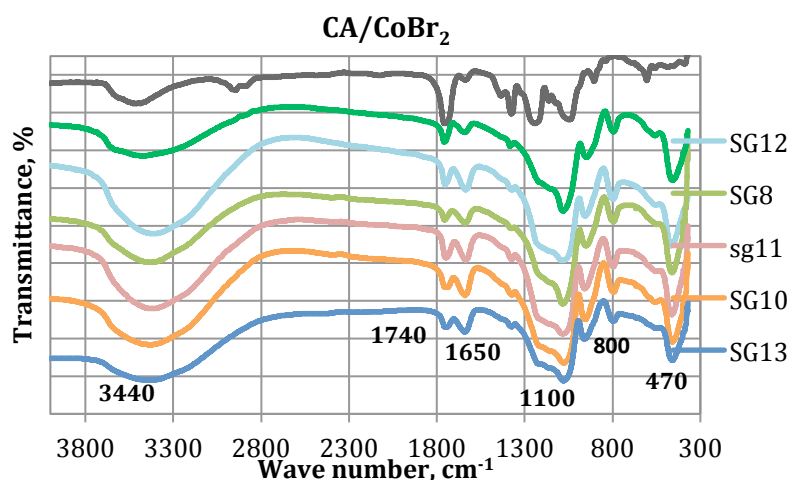


Figure 22 FTIR spectra for CoBr₂/CA/SiO₂ composite before carbonization.

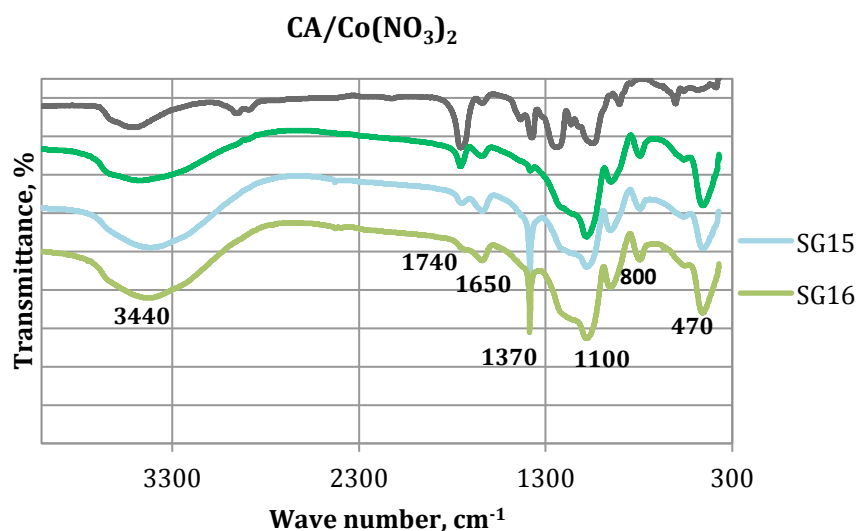


Figure 23 FTIR spectra for Co(NO₃)₂/CA/SiO₂ composite before carbonization.

5.2 Carbonization of precursor containing xerogels

Xerogel samples (regardless to polymeric precursor) carbonized at 800 °C have uniform black colour which points to uniform distribution of precursor within the volume of gel.

5.2.1 Carbonization of HPC containing composites.

Surface of samples carbonized without preliminary grinding despite loss of transparency remain glossy as in precursor xerogels. Color of samples carbonized after grinding to powder was slightly lighter than that of monolithic samples. Results of TGA showed that powder samples are characterized by greater weight loss than monolithic samples (Figure 24), which is consistent with difference in color of samples. The TGA curve shows that cellulose degraded in three steps, which were suggested by Chatterjee as representing the thermal degradation of the cellulosic materials [30]. The first step represents the evolution of the volatile matter or dehydration that ends at ~350°C. The second step represents the main thermal degradation of cellulose. The third step represents the carbonization of the products, which starts around 500°C.

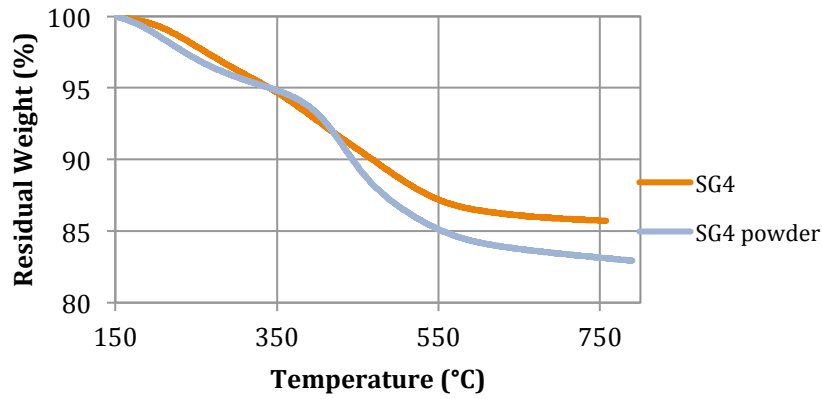


Figure 24 TGA of SG4 samples carbonized in powder and monolith condition.

i) Low temperature nitrogen sorption isotherms of carbon composite samples synthesized from HPC containing gels.

Results from measurements of low-temperature nitrogen sorption are presented in Figure 25-26 and Table 1.

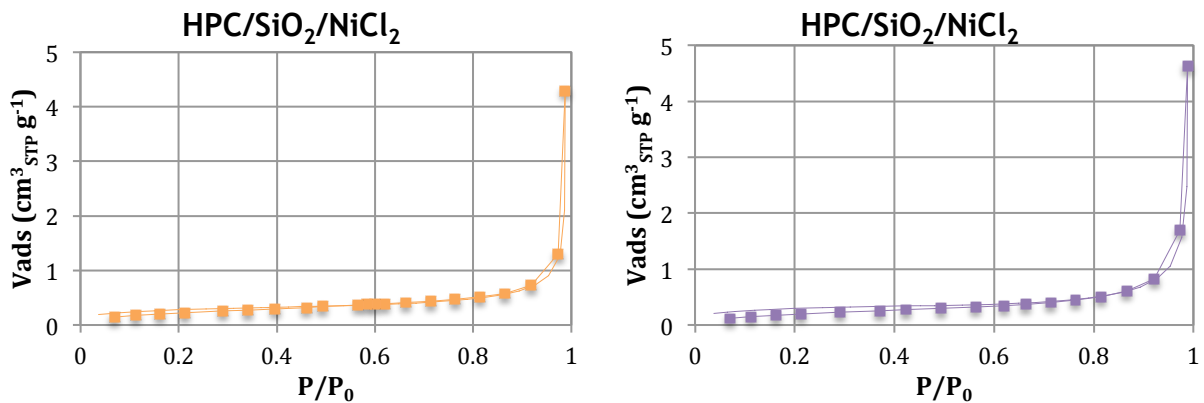


Figure 25 Low temperature nitrogen sorption isotherms of carbon composite sample SG1 and SG2

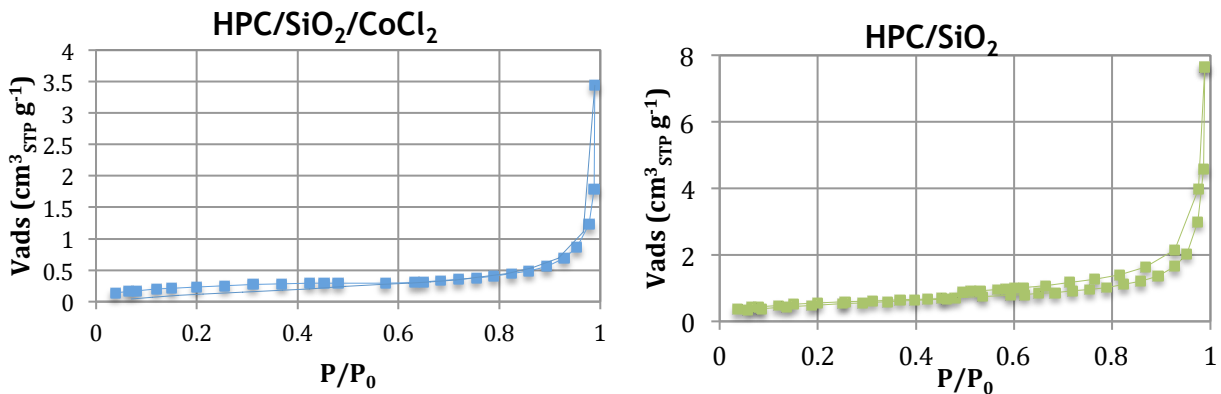


Figure 26 Low temperature nitrogen sorption isotherms of carbon composite sample SG3 and SG4

These isotherms exhibit type II, typical to multilayer and physical adsorption that can occur in non-porous solids. Type II isotherms are characterized by two inflections, a relative pressure values lower than 0.1 and higher than 0.9. The first inflection is considered as indicating the fill of the first adsorbed layer.

The specific surface area and micropore volume calculated from the Low-temperature nitrogen sorption isotherms is presented at Table 1.

Table 1 Textural characteristics of C/SiO₂ samples synthesized from HPC containing xerogels .

Sample	Salt	Appearance	Metal/HPC weight ratio	HPC/SiO ₂ weight ratio	BET Surface Area (m ² g ⁻¹)	Microcopore volume (cm ³ g ⁻¹)
SG1	NiCl ₂	Powder	0.3	0.3	0	-
		Monolith			1	-
SG2	NiCl ₂	Powder	0.2	0.15	1	-
SG3	CoCl ₂	Powder	0.2	0.15	1	-
SG4	-	Powder	-	0.15	1	-
		Monolith			2	-

These results show that the materials are nonporous. Therefore, the external surface of the particles is mainly where the adsorption occurs. The difference between specific surface area values in monolithic and powder form can be neglected. In HPC samples containing composites the value for specific surface area is low which could be caused by collapse of porous structure during gel drying.

As it could be seen samples with HPC are characterized by small amount of macro and mesopores (Figure 27-28).

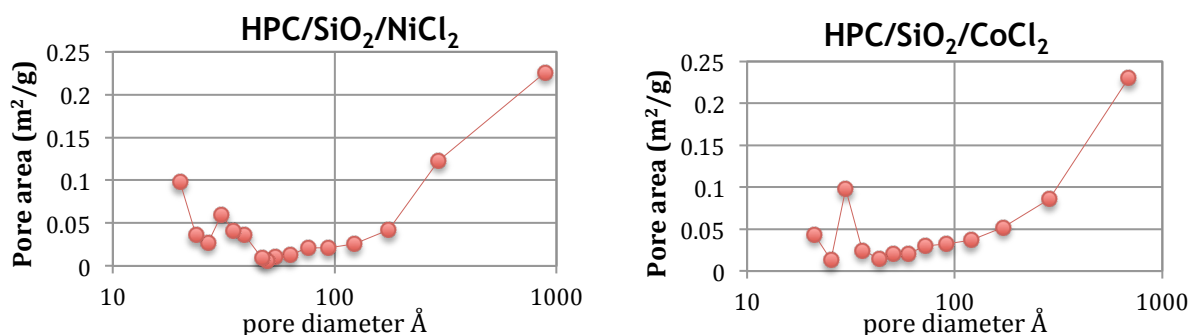


Figure 27 Pore size distribution of carbon composite sample SG1 (left) and SG3 (right)

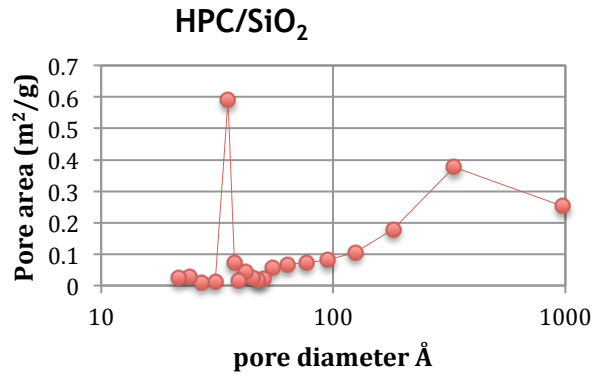


Figure 28 Pore size distribution of carbon composite sample SG4

ii) SEM of carbon samples synthesized from HPC containing gels.

The SEM investigation of sample SG1 showed that this sample does have neither macropores nor mesopores (Figure 29), which is consistent with the results of low temperature nitrogen sorption these images can also demonstrate the presence of crystals with size of 50-300nm on the sample surface which means that a uniform coating was not obtained.

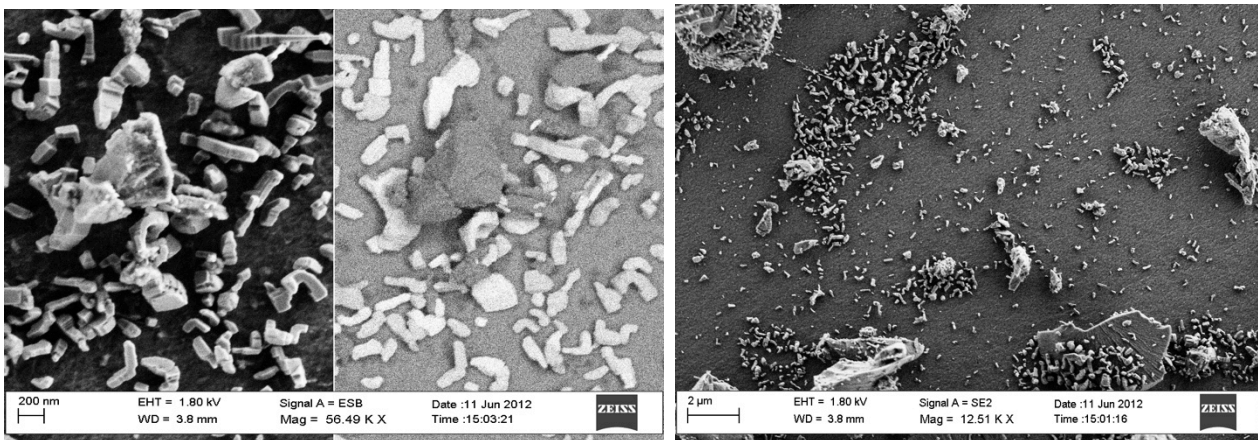


Figure 29 SEM images of the SG1 sample (HPC with nickel)

The SEM investigation of sample SG4 showed that these samples do not have macropores or mesopores (Figure 30), which is consistent with the results of low temperature nitrogen sorption

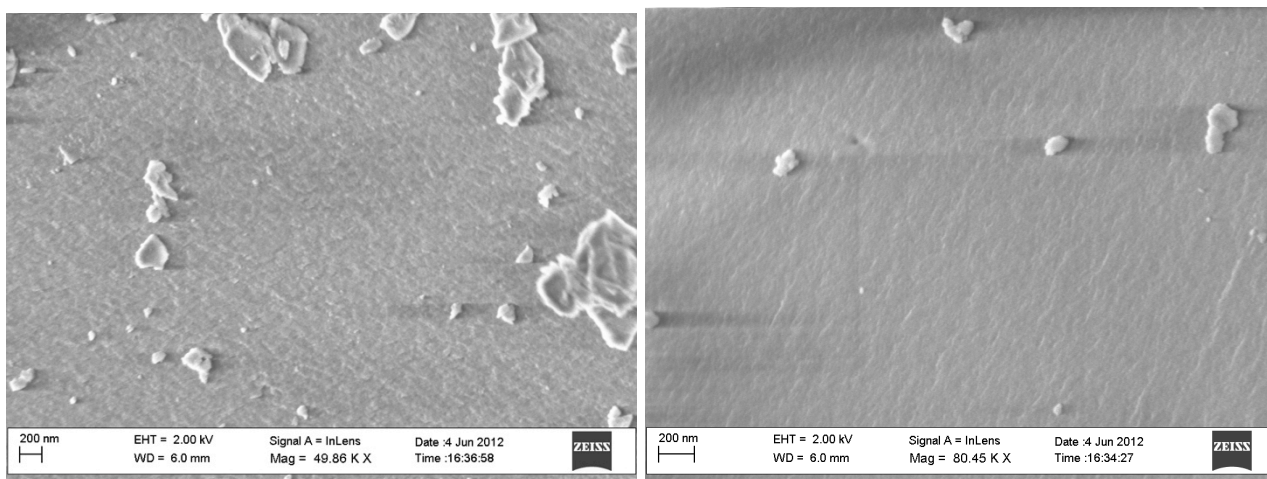


Figure 30 SEM images of the SG4 sample (HPC without salt)

iii) X-Ray Diffraction of carbon composite samples synthesized from HPC containing gels.

XRD analysis for sample SG1 (Figure 31) showed the presence of metallic nickel. Thus crystals present on the surface of the samples are most probably consisting of Ni.

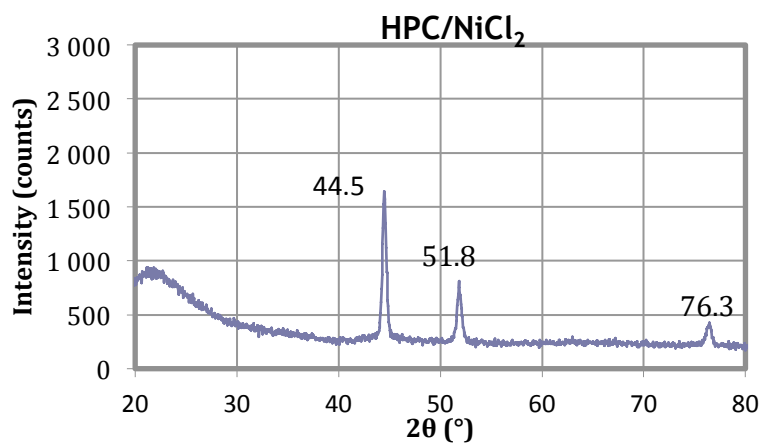


Figure 31 The X-ray diffraction patterns of carbon composite with HPC/NiCl₂

5.2.2 Carbonization of CA containing composites.

The presence of cellulose acetate contributed considerably to the increase of specific surface area in carbonized samples comparing with HPC derived samples. Consequently, it is possible to relate that the transparent gels obtained by HPC do not show large specific surface area, in contrast to opaque gels.

- i) Low temperature nitrogen sorption isotherms of carbon composite samples synthesized from CA containing gels.

The isotherms exhibit typical shape of type IV isotherm (Figure 32-37). Type IV isotherms have a high level at higher pressure which could point to the presence of mesoporous.

These samples exhibit steep capillary condensation (hysteresis loop) indicating that these samples have mesopores of a larger size.

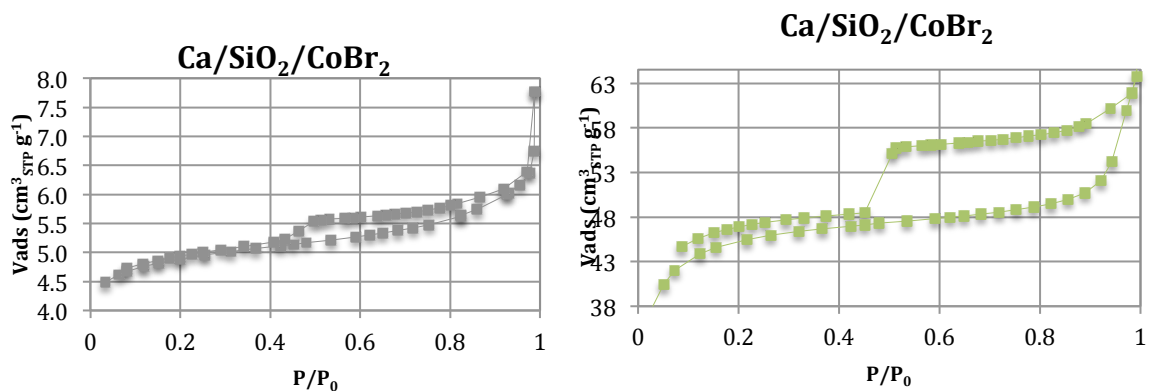


Figure 32 Low temperature nitrogen sorption isotherms of carbon sample SG5 (left) and SG8 (right)

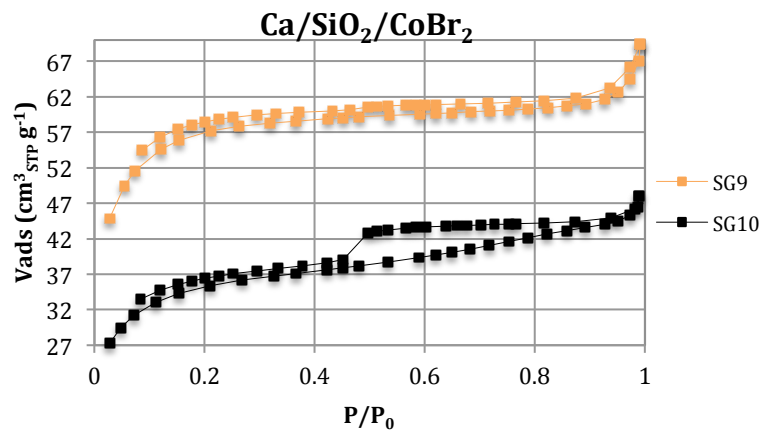


Figure 33 Low temperature nitrogen sorption isotherms of carbon sample SG9 (orange) and SG10 (black)

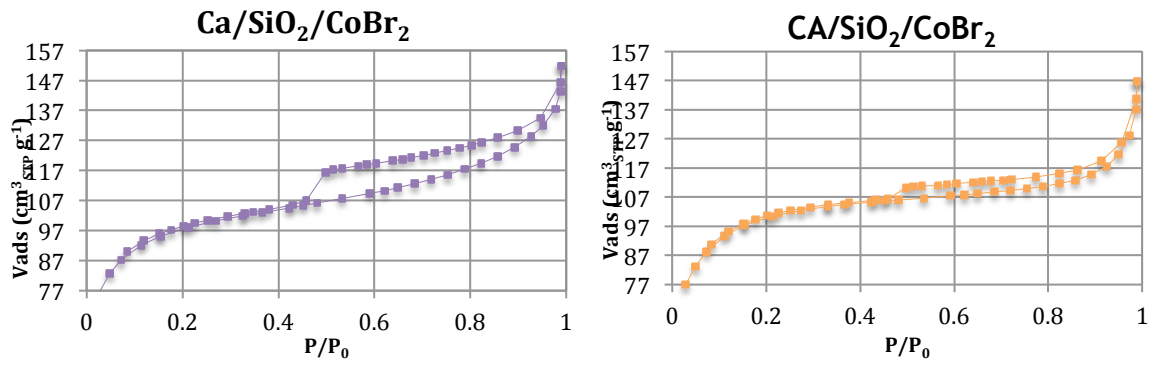


Figure 34 Low temperature nitrogen sorption isotherms of carbon sample SG11 and SG12

In some samples is observed low pressure hysteresis. The capillary condensation hysteresis loops are more pronounced, and close at a lower relative pressure.

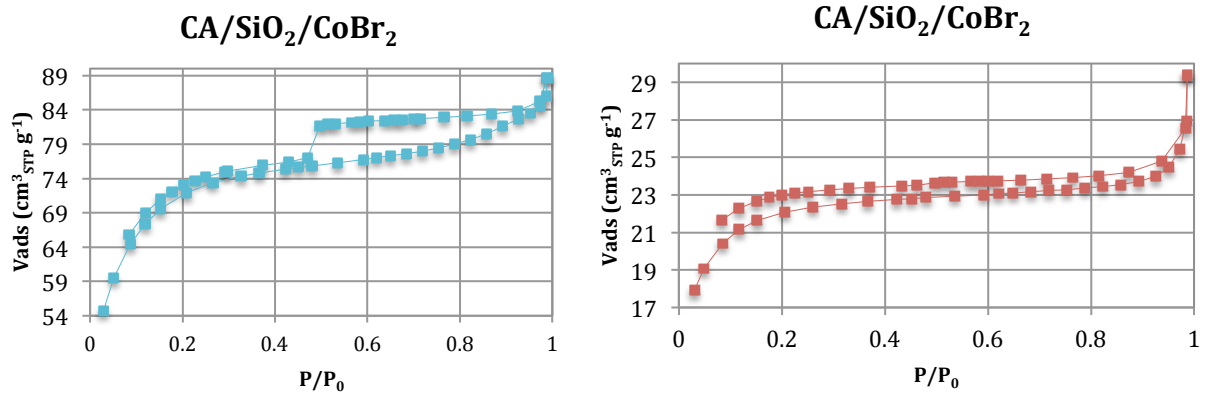


Figure 35 Low temperature nitrogen sorption isotherms of carbon sample SG13 (left) and SG14 (right)

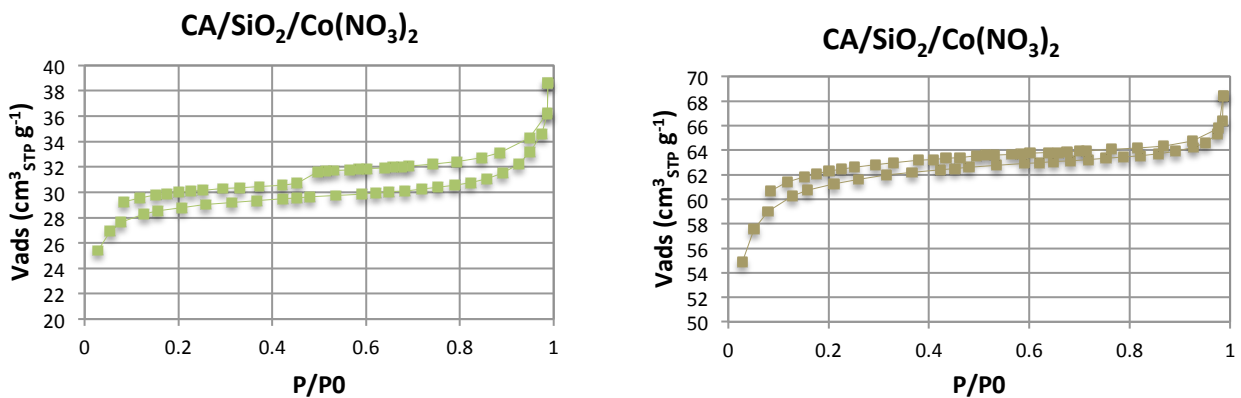


Figure 36 Low temperature nitrogen sorption isotherms of carbon sample SG15 (left) and SG16 (right)

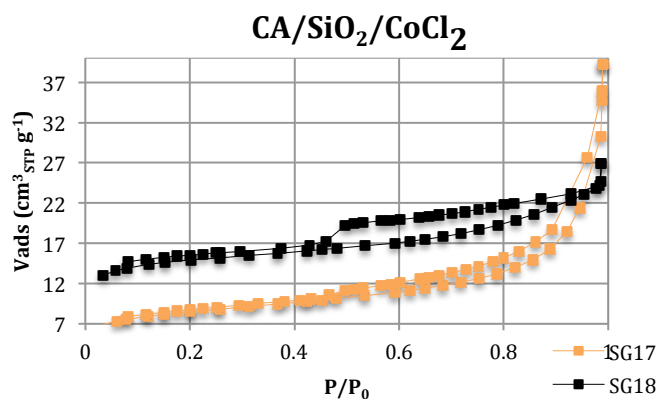


Figure 37 Low temperature nitrogen sorption isotherms of carbon sample SG17 and SG18

In general, the isotherms were very similar for the different concentrations.

The simultaneous addition of cobalt bromide, acetate cellulose and acetone as solvent made possible to prepare amorphous carbon materials with surface area value up to 346.5 m² g⁻¹, taking a gelation time of five days. One possible reason for this result can be the specific interaction between the cobalt bromide and the cellulose acetate that can result in complexes formation. These complexes can improve the porous structures of the material.

Table 2 Textural characteristics of carbonized CA containing xerogels.

Sample	Salt		Metal/C A weight ratio	CA/SiO ₂ ratio	BET Surface Area (m ² g ⁻¹)	Microcopore volume (cm ³ g ⁻¹)
SG5	CoBr ₂	Powder	0.1	0.3	17	-
SG6	CoBr ₂	Powder	0.1	0.3	16	-
SG7	CoBr ₂	Powder	0.1	0.4	111	0.03
SG8	CoBr ₂	Powder	0.2	0.15	153	0.05
		Monolith	0.2	0.15	1	-
SG9	CoBr ₂	Powder	0.2	0.3	196	0.06
SG10	CoBr ₂	Powder	0.2	0.3	122	0.03
SG11	CoBr ₂	Powder	0.2	0.3	336	0.1
SG12	CoBr ₂	Powder	0.2	0.3	347	0.1
SG13	CoBr ₂	Powder	0.3	0.4	249	0.09
SG14	CoBr ₂	Powder	0.4	0.15	76	0.02
SG15	Co(NO ₃) ₂	Powder	0.2	0.3	97	0.03

SG16	Co(NO ₃) ₂	Powder	0.2	0.15	206	0.08
		Monolith	0.2	0.15	3	-
SG17	CoCl ₂	Powder	0.2	0.3	30	0.006
SG18	CoCl ₂	Powder	0.2	0.3	51	0.02
SG19	CoCl ₂	Powder	0.2	0.15	4	-

From Table 2 could be seen that the sample SG12 demonstrates almost the same value for surface area as SG11. Sample SG12 differs from sample 11 by the heating time and mixing solution. One could conclude that 1 hour of stirring is sufficient for preparation of sol.

Decreasing the amount of precursor in the sample (sample 18 comparing to samples 11 and 12) leads to decreasing of the surface area. Sample SG5 show smaller value of specific surface area comparing with samples SG11 and SG12 that have more volume of metal. On the one hand in case of material formed from cobalt bromide, less quantity of metal significantly affected the value of specific surface area. On the other hand, the influence of twice less volume of carbon precursor changed the value of the specific surface area for almost twice less value.

Decreasing of the amount of water in the sample (sample SG11 comparing with sample SG9) leads to increasing of the surface area and micropore volume as was expected [16].

In case of materials formed from cobalt chloride SG17 showed similar value of specific surface area comparing with SG18 and this sample was prepared with 5hours of reaction.

These results showed that samples carbonized in powder form present higher value of specific surface area than samples carbonized in monolith form (Table 2). The possible reason for this effect could be that the powder form of the sample leads to easier removal of volatile components during carbonization, which leads to opening of porosity and increasing of surface area.

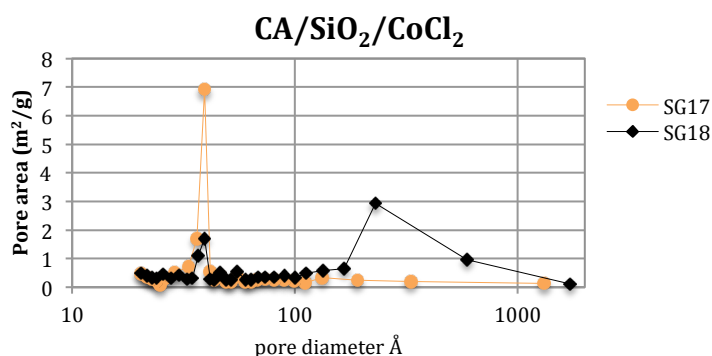


Figure 38 Pore size distribution of carbon composite sample SG17 and SG18

As can be seen (Figure 38) samples SG17 and SG18 show the presence of both mesopores and macropores.

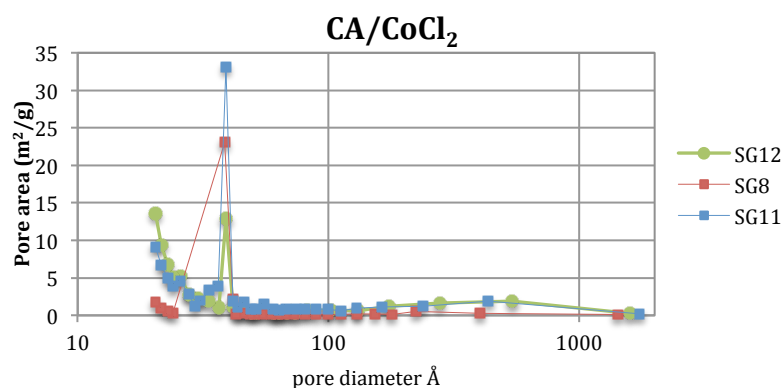


Figure 39 Pore size distribution of carbon composite sample SG11, SG12 and SG8

The distributions of pore size for SG11 SG12 and SG8 can be seen in Figure 39 and are very similar. This distributions show homogenous distribution of mesopore.

ii) SEM images of carbon composite samples synthesized from CA containing gels.

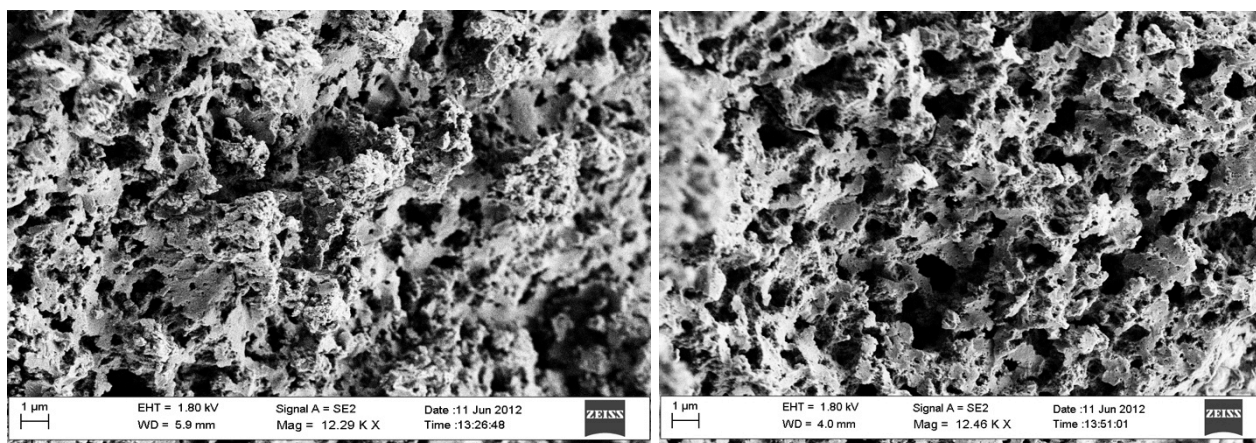


Figure 40 SEM images of the sample SG11 (left) and SG12 (right).

Secondary electron detectors were used for the topography investigation. As it can be seen Figure 40, the SEM micrographs for sample SG11 and SG12 are very similar and the distribution of pores is homogeneous. These pictures show that they are mesoporous materials, which is consistent with isotherm type IV and presence of hysteresis (Table 2, Figure 34).

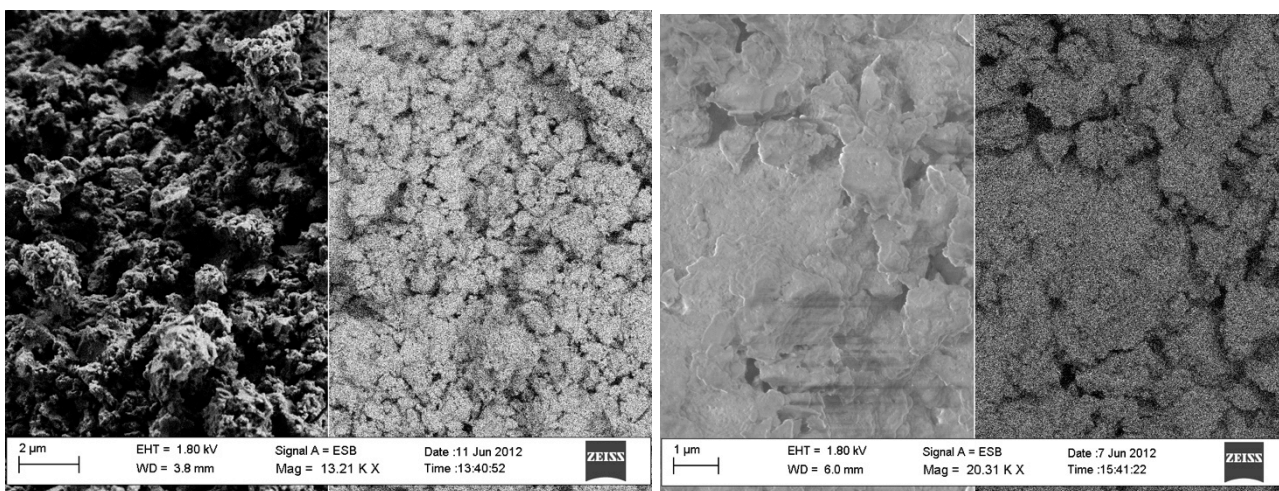


Figure 41 SEM images of the SG11 (left) and SG12 (right)

The method of separating and detecting the backscattered electrons is called: Energy selective Backscattered detection (ESB). ESB detector was used for topography investigation in order to see compositional contrast on the surface of samples. The results are present in Figure 41 and as it can be seen, there are no crystals in the top layer, which could point to homogeneous distribution of cobalt in material.

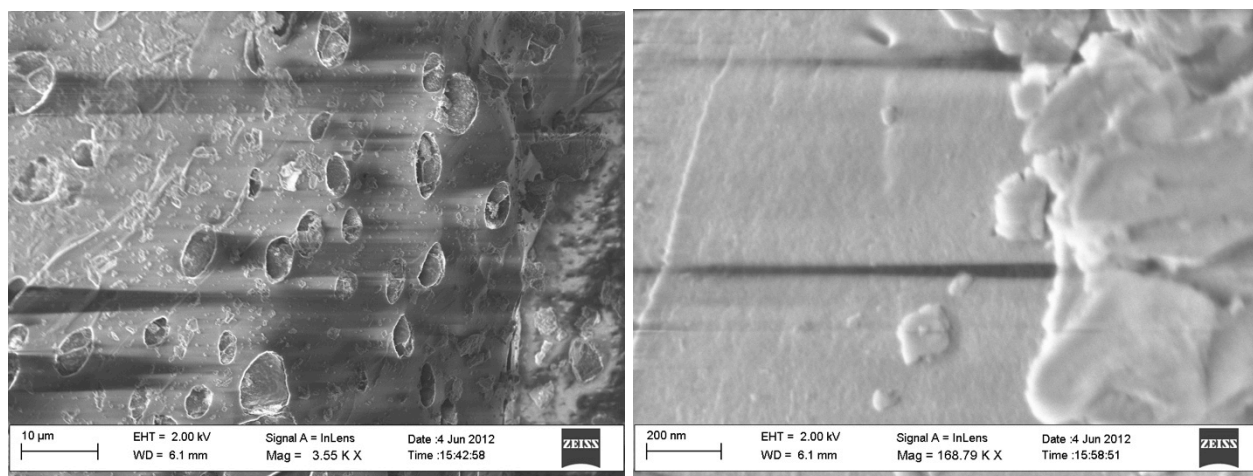
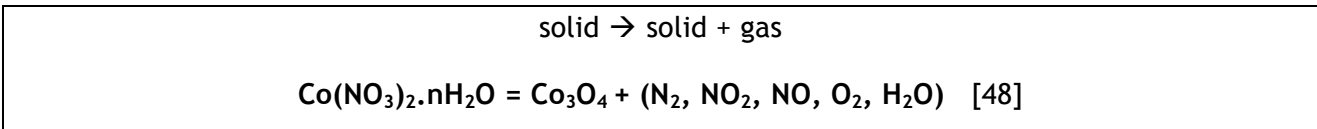


Figure 42 SEM images of the sample SG16 monolith and SG16 powder

According to SEM analysis sample SG16 carbonized without preliminary grinding (Figure 42) has macropores with diameter of 2-7 μm while sample SG16 carbonized in the powder form does not show any macro or mesoporosity, which is consistent with results of low-temperature nitrogen sorption according to which carbon material synthesized by carbonization of SG16 powder is mainly microporous material (Table 2, Figure 36). Presence of macropores in carbon material synthesized from monolithic SG16 could be the most probably caused by fast formation of NO₂ and O₂ during thermal decomposition (Equation 4). Pressure created by evolved gases most

probably caused "microexplosions" and formation of cavities in the material. When using powdered precursor, particles of sample are small and quantity of cobalt nitrate is not enough to destroy structure of material. Simultaneously powder form of sample leads to easier removing of volatile components during carbonization which leads to opening of porosity and increasing of surface area.

The thermal decomposition of Co(NO₃)₂ is a characteristic heterogeneous reaction of the type:



Equation 4 The thermal decomposition of Co(NO₃)₂

Is it generally assumed that the decomposition of Co(NO₃)₂ hydrates involves a dehydration stage, followed by decomposition of anhydrous Co(NO₃)₂ proceeds in stages.

Secondary electron detectors were used for the topography investigation for sample SG17 and SG18 as can be seen in Figure 43-44.

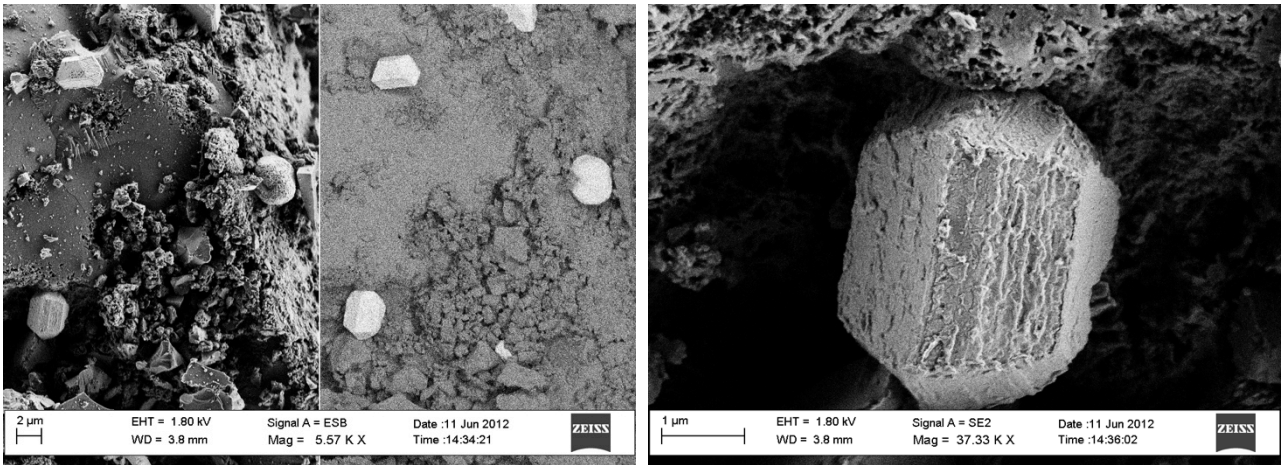


Figure 43 SEM images of the of sample SG17

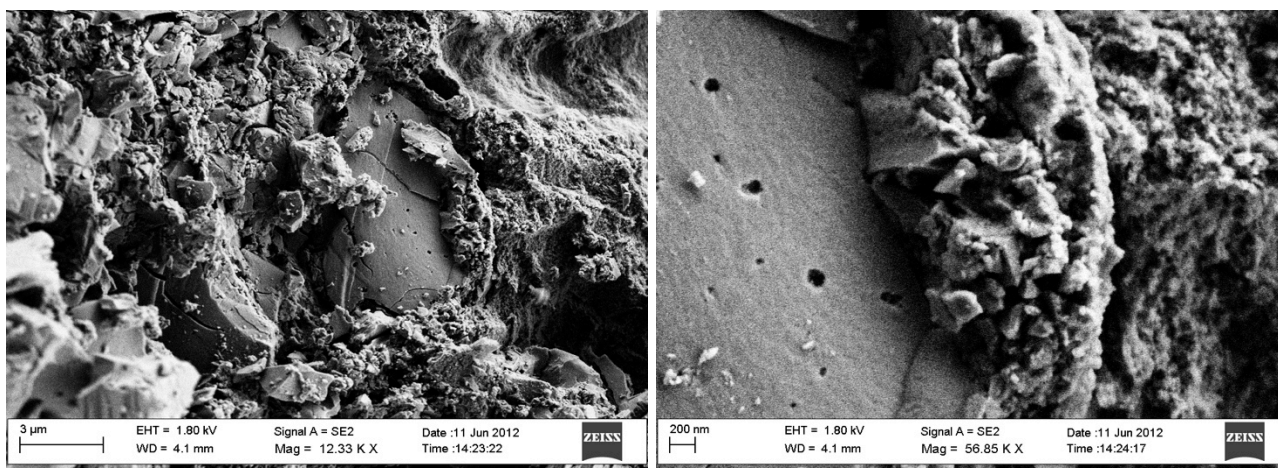


Figure 44 SEM images of the of sample SG18

As it can be seen, there is a lot of large crystals in the top layer (Figure 43 (left)), which means that a nonuniform coating of cobalt was obtained.

Moreover, using a SEM with a higher magnification, it was possible to detect more clearly the geometry of the crystals, as can be seen in Figure 43 (right).

iii) X-Ray Diffraction of carbon composite samples synthesized from CA containing gels.

The XRD patterns for samples synthesized by carbonization of CA in the presence of CoBr₂ (Figure 45) and CA/CoCl₂ (Figure 46) are very similar and display four peaks at 2θ=44.9, 52.4, 77.4 and 91°. These peaks show the presence of metallic cobalt in composites. In thermal decomposition of CoBr₂ and CoCl₂ oxide cobalt can be form as was expected with Equation 4. However, in this case it worth noting that cobalt oxide is not observed since during carbonization volatile compounds must diffuse out of the system.

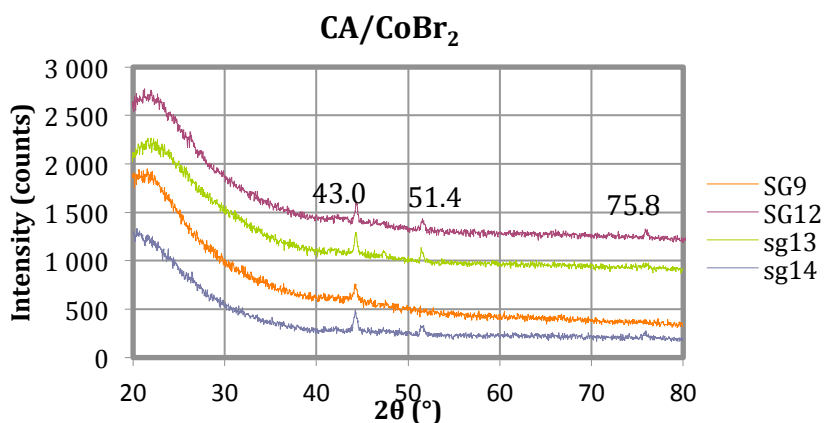


Figure 45 X-ray diffraction patterns of carbon material: CA/CoBr₂ samples

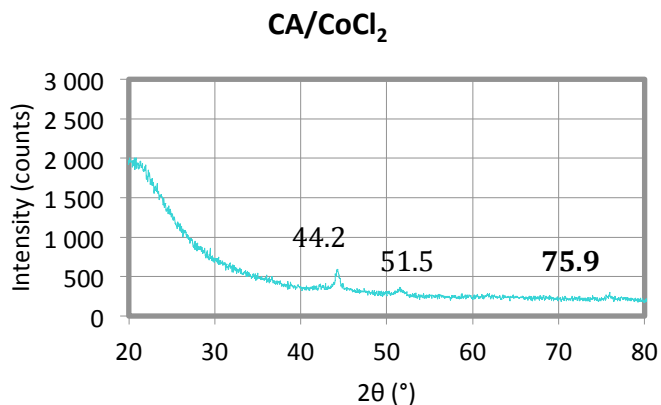


Figure 46 X-ray diffraction patterns of carbon material: CA/CoCl₂ sample

XRD patterns of carbonized samples SG15 and SG16 (Co(NO₃)₂ was used as pre-catalyst) are characterized by weak and broad peaks (Figure 47) that could be assigned to highly dispersed metallic Co.

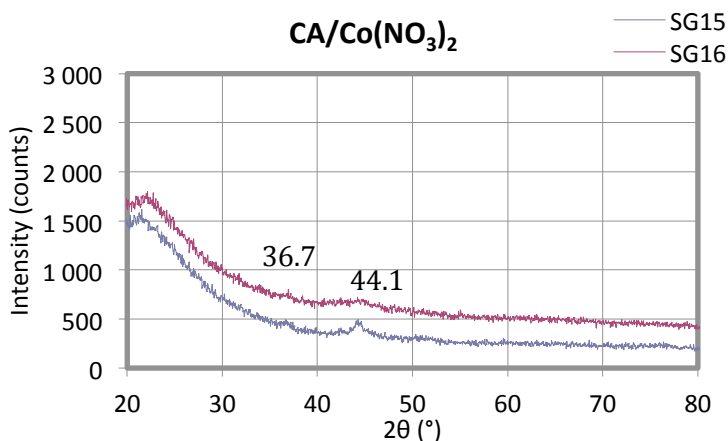


Figure 47 X-ray diffraction patterns of carbon material: CA/Co(NO₃)₂ samples

5.3 Discussion

The objectives proposed for this work were achieved and the timeline for this project can be found in Appendix (Table A6).

Salt of 3d metals affect process of gelation. HPC containing silica xerogels without salts was prepared in 7 - 90 days while HPC containing silica xerogel with salts were prepared in 6 days in oven and in 60 days without ageing. CoBr₂ displayed the highest influence on the rate of gelation of CA containing silica gels since gelation occurs in 5-15 days.

Ni/Co/SiO₂ composites were prepared by carbonization of HPC/CA containing silica xerogel and the carbonization of HPC containing xerogel resulted in nonporous materials. However, carbonization of CA containing xerogels resulted in porous materials with specific surface areas between 30-346 m² g⁻¹ (Table 2). Results obtained could be explained by different interaction between different cellulose derivatives and Ni(II) and Co(II) salts resulting in the formation of complexes with different morphology which led consequently to different morphology of gels and xerogels.

The most probable anion in salt is also very important for the gel formation. Formation of different complexes by Co(NO₃)₂ and CoBr₂ could explain differences in specific surface area and morphology of carbonized composites comparing to samples containing CoCl₂ (Table 2)

Ni/Co/SiO₂ composites that were synthesized by carbonization of CA could be prospective for the synthesis of hydrogen storage and supercapacitors materials.

Nonporous HPC containing xerogels obtained in our work could be prospective for the preparation organic/inorganic hybrid film, for different applications. These materials can be used to increase the mechanical and thermal properties and for the preparation of unique composites [25].

6 Conclusions

HPC and CA containing silica gels in presence of Co(II) and Ni(II) salts were prepared through sol-gel approach using TEOS as silica precursor.

It was revealed that Co(II) and Ni(II) salts affect process of gelation. Precursor containing silica xerogels without salts were prepared in 7 - 90 days while HPC containing silica xerogels with salts were prepared in 6 days in oven and in 60 days without ageing. CoBr₂ displayed the highest influence on the rate of gelation of CA containing silica gels: gelation occurs in 5-15 days.

Ni/Co/SiO₂ composites were prepared by carbonization of HPC(CA) containing silica xerogels. Carbonization of HPC containing xerogels resulted in non porous materials. Carbonization of CA containing xerogels resulted in porous structure material with specific surface area values between 30-346 m² g⁻¹

Concentration of components has nonlinear influence in values of specific surface area of Ni/Co/SiO₂ composites;

Ni/Co/SiO₂ composites that were synthesized by carbonization of CA/HPC could be prospective for the synthesis of hydrogen storage and supercapacitors.

6.1 Other work performed

This project was a challenge with several critical questions and issues in order to adjust the theory and practical situations about synthesis of nanostructured composites with high surface area and metal salts incorporated.

Before the final protocol for the synthesis of precursor containing gels was established, some parameters known to affect the pore size and surface area were adjusted. They are pH of the initial mixture and drying conditions. Both basic and acid catalysis were considered to be use in our work (table A4), basic catalyst was chosen to be ammonia hydroxide. The experiments made with basic catalyst did not work, because the Co(II) and Ni(II) salts form non soluble precipitates most probably because of formation of amino complexes. Thus all samples were prepared only in the presence of HCl as catalyst (see section 4 and 5).

Freeze drying technique was tested for drying process. Since freeze-drying could be effective to prevent the porous structure from shrinking because the solvent in the pores is removed by sublimation under vacuum and consequently the capillary force does not exert on the porous structure [49, 50]. Since gels samples prepared in our work contained large amount of ethanol or acetone, freeze-drying led to boiling of dispersion medium (because freezing point of ethanol is below the operating temperature -50°C) and collapse of porous structure.

6.2 Future work

1. Optimization of the sol-gel parameters in order to improve the final structure of the material and to increase the specific surface area.
2. A further study of the influence of concentration of reagents, conditions of aging and gelation on the porous structure of the final Ni(Co)/C/SiO₂ composites .
3. Investigation of the structure of samples with TEM.
4. Investigation of hydrogen storage capacity of synthesized materials

6.3 Final appreciation

In the beginning of this Erasmus experience I had a few rough days since I left my friends, my family and comfort in Portugal. But then being in a different environment, I found myself taking on challenges I would never have done at home.

This experience taught me to act independently and was very positive since it contributed so much for my autonomy. In five months I was exclusively dedicated to this project, putting all my dedication in this work. I remember the places that I visited but, to be honest, I spent most of my time in the lab, and I really enjoyed my research.

During this time, I was in several meetings with my group work where I presented my results a lot of times. At the end, I completed my project and presented my results during the defense of my thesis and I got very positive feedback from people.

7 References

1. http://news.cnet.com/8301-11128_3-20017972-54.html. [cited 2012].
2. G. Q. Lu, X. S. Zhao, *Nanoporous materials - an overview*. Series on Chemical Engineering. Vol. 4. 2004.
3. Jinwoo Lee, Sangjin Han, Taeghwan Hyeon, *Synthesis of new nanoporous carbon materials using nanostructured silica materials as templates*. Journal of Materials Chemistry, 2004. **14**: p. 478-486.
4. J. Rouquerol, D. Avnir, C.W. Fairbridge, D.H. Everett, J.H. Haynes, N. Pericone, J.D.F. Ramsay, K.S.W. Sing, K.K. Unger, *Pure and Appl. Chem*, 1994. **66**: p. 1739-1758.
5. Willems & van den Wildenberg (W&W), *ROADMAPS AT 2015 ON NANOTECHNOLOGY APPLICATION IN THE SECTORS OF: MATERIALS, HEALTH & MEDICAL SYSTEMS, ENERGY, R.R.o.N. materials*, Editor 2005. p. 13-20.
6. Whitesides, G.M., *Self-assembly and nanotechnology*. Proc. SPIE, 1996. **2716**(Smart Structures and Materials 1996: Smart Materials Technologies and Biomimetics, San Diego, CA,): p. 307-308.
7. Ryong Ryoo, Sang Hoon Joo, and Shinae Jun, *Synthesis of Highly Ordered Carbon Molecular Sieves via Template-Mediated Structural Transformation*. The journal of physical chemistry, 1999. **103**: p. 7743-7746.
8. C.O. Nwokem, N.C. Nwokem, *Development and Studies on Deferrated-Kaolinite-Template Porous Carbons from Furfuryl alcohol*. Researcher, 2010. **2**(7): p. 21-26.
9. Farook Adam, Jeyashelly Andas and Ismail Ab. Rahman, *The synthesis and Characterization of Cobalt-Rice Husk Silica Nanoparticles*. The Open Colloid Science Journal, 2011. **4**: p. 12-18.
10. Malsch, I., *Nanotechnology helps solve the world's energy problems*, 2003: <http://www.nanoforum.org>.
11. Skowronski, J.M., *Effect of nickel catalyst on physichemical properties of carbon xerogels as electrode materials for supercapacitor*. Current Applied Physics, 2012. **12**(3): p. 911-918.

12. F. Lufrano, P.S., *Mesoporous Carbon Materials as Electrodes for Electrochemical Supercapacitors*. International Journal of Electrochemical Science, 2010. **5**: p. 903-916.
13. http://www.aist.go.jp/aist_e/aist_today/2007_23/nanotec/nanotec_08.html. [cited 2012].
14. <http://sun77a.blogspot.se/2010/12/carbon-age-dark-element-brighter-future.html>. [cited 2012].
15. Iler, R.K., *The Chemistry of Silica*, ed. Wiley 1979, New York.
16. C. J. Brinker, G.W.S., *Sol-Gel Science: The physics and Chemistry of Sol-Gel processing* 1990, New York: Academic Press.
17. Huifang Xu, H.Z., Yudong Huang, Yang Wang, *Porous carbon/silica composites monoliths derived from resorcinol-formaldehyde/TEOS*. Journal of Non-Crystalline Solids, 2010. **356**(971-976).
18. Chunling Liu, Sridhar Komarneni, *Carbon-silica xerogel and aerogel composites*. Journal of porous materials, 1995. **1**: p. 75-84.
19. Hench, L.L., Orefice R. L., *Sol-Gel Technology*. Kirk-Othmer Encyclopedia of Chemical Technology 1997, New York: John Wiley and Sons.
20. Wright, J.D., Sommerdijk, N.A.J.M, *Sol-Gel materials: Chemistry and applications* 2001, London: Taylor & Francis books Ltd.
21. Jae Chul Ro and J.C. In, *Structures and properties of silica gels prepared by the sol-gel method*. Journal of Non-Crystalline Solids, 1991. **130**(1): p. 8-17.
22. Klemm D, H.B., Fink HP, Bohn A., *Cellulose: fascinating biopolymer and sustainable raw material*. Angewandte Chemie, 2005. **44**(22): p. 3358-93.
23. Sequeira, S., Evtuyugin, D., Portugal, I., *Synthesis and Structural Characterization of Cellulose/Silica Hybrids Obtained by Heteropolyacid Catalysed Sol-Gel Process*. Materials, Chemicals, and Energy from Forest Biomass. Vol. 8. 2007.
24. Yano S., *Preparation and Characterization of Hydroxypropyl Cellulose/Silica Microhybrids*. Polymer, 1994. **35**: p. 5565-5570.
25. Shojaie, S.S., Rials, T.G., Kelly, S.S., *Preparation and Characterization of Cellulose Acetate Organic-Inorganic Hybrid Films*. The Journal of Applied Polymer Science, 1995. **58**: p. 1263-1274.

26. R. A. Zoppi, M.C.G., *Hybrids of cellulose acetate and sol-gel silica: Morphology, thermomechanical properties, water permeability, and biodegradation evaluation*. Journal of Applied Polymer Science, 2002. **84**(12): p. 2196-2205.
27. Rita S. Werbowyj, Derek G. Gray, *Ordered phase formation in concentrated Hydroxypropylcellulose solutions*. Macromolecules, 1980. **13**: p. 69-73.
28. I. Bobowska, P.W., T. Halamus, *Organic-Inorganic nanocomposites of (2-hydroxypropyl)cellulose as a precursor of nanocrystalline zinc oxide layers*. Polymers for Advanced Technologies, 2008. **19**(1860).
29. Esther G. Calvo, J. Ángel Menéndez, Ana Arenillas, *Designing Nanostructured Carbon Xerogel 2011*, Spain.
30. M.C., C.P.K.a.C., *Thermogravimetric analysis of cellulose*. Journal of Polymer Science, 1968. **6**: p. 3217-3233.
31. Baumann T F, F.G.A., Satcher J H, Yoshizawa N, Fu R, Dresselhaus M S, *Synthesis and Characterization of copper doped carbon aerogel*. Langmuir, 2002. **18**: p. 7073.
32. Fu R, Y.N., Dresselhaus MS, Dresselhaus G, Satcher JH, Baumann T., *The XPS study of copper-doped carbon aerogels*. Langmuir, 2002. **18**(10100): p. 4.
33. L. Zubizarreta, J.A.M., N. Job, F. P. Marco-Lozar, J. P. Pis, A. Linares-Solano, D. Cazorla-Amorós, A. Arenillas, *Ni-doped carbon xerogels for H₂ Storage*. Carbon, 2010. **48**: p. 2722-2733.
34. Dinega DP, B.M., *A solution-phase chemical approach to a new crystal structure of cobalt*. Angewandte Chemie International 1999. **38**: p. 1788-1791.
35. Puentes, V.F., Krishnan, K. M. & Alivisatos, *Colloidal nanocrystal shape and size control: the case of cobalt*. Science, 2001. **291**: p. 2115-2117.
36. Hyeon T, C.Y., Park J, Lee SS, Kim YW, *Synthesis of Highly Crystalline and Monodisperse Cobalt Ferrite Nanocrystals*. The Journal of Physical Chemistry B, 2002. **106**(27): p. 6831-6833.
37. Harrington, P.J. In *Transition Metals In Total Synthesis*; Wiley: New York, 1990; p 259.
38. Soo-Jin Park, S.-Y.L., *A study on hydrogen-storage behaviors of nickel-loaded mesoporous MCM-41*. Journal of Colloid and Interface Science, 2010. **346**(1): p. 194-198.
39. Sing, K.S.W., Everett, D. H., Haul, R. A. W., Moscou, L, Pierotti, R. A., Rouquerol, J. and Siemieniewska, T. , *Reporting physical adsorption data for gas/solid systems with*

- special reference to the determination of surface area and porosity.* Pure & Applied Chemistry, 1985. **57**: p. 603-619.
40. Stephen Brunauer, P.H.E., Edward Teller, *Adsorption of Gases in Multimolecular Layers.* Journal of the American Chemical Society, 1938. **60**(2): p. 309-319.
 41. Eric Lifsthin, *X-ray Characterization of Materials*, ed. Wiley-VCH 1999, New York.
 42. Nahla A. El-Wakil, Y.F., Ragab E. Abou-Zeid, Alain Dufresne, and Samya El-Sherbiny *Liquid crystalline behavior of hydroxypropyl cellulose esterified with 4-alkoxybenzoic acid.* BioResources, 2010. **5**(3): p. 1834-1845.
 43. Beganskienė Aldona, S.V., Kurtinaitienė Marytė, Juskėnas Remigijus, Kareiva Aivaras, *FTIR, TEM and NMR investigations of Stober Silica Nanoparticles.* Materials Science, 2004. **10**: p. 1392-1320.
 44. Abdel-Hadi, A.K., *Monomeric dioxouranium(VI), chromium(III), cobalt(II), nickel(II) and copper(II) complexes with primary cellulose acetate (PCA).* Cellulose, 1995. **2**: p. 235-241.
 45. Rodriguez K, R.S., Gatenholm P, *Biomimetic calcium phosphate crystal mineralization on electrospun cellulose-based scaffolds.* APPLIED MATERIALS & INTERFACES, 2011. **3**: p. 681-689.
 46. G. D. Chukin, V.I.M., *Infrared spectra of silica.* Journal of Applied Spectroscopy, 1977. **26**(2): p. 223-229.
 47. Naboka, O.S.-V., Anke; Lundgren, Per; Enoksson, Peter; Gatenholm, Paul, *Cobalt (II) Chloride Promoted Formation of Honeycomb Patterned Cellulose Acetate Films.* . Journal of Colloid and Interface Science, 2012. **367** (1): p. 485-493.
 48. A. Matecki, A.M., R. Gajerski, B. Prochowska-Klisch, A. Podgórecka, *The mechanism of thermal decomposition of Co(NO₃)₂ · 2H₂O* Journal of Thermal Analysis and Calorimetry, 2005. **34**(1): p. 203-209.
 49. Tamon, H., Ishizaka, H. Yamamoto, T. and Suzuki, T., *Preparation of mesoporous carbon by freeze drying.* Carbon, 1999. **37**: p. 2049-2055.
 50. Tamon, H., Ishizaka, H., *Preparation of organic mesoporous gel by supercritical/freeze drying.* Drying Technology, 1999. **17**: p. 1653-1665.

8 Appendix

Table A1 composition of precursor/SiO₂ samples

Sample	Precursor	Co(Ni) Salt	Precursor/SiO ₂ weight ratio	metal / precursor weight ratio	H ₂ O/TEOS (mol)	W(SiO ₂)% wt/vol
SG1	HPC	NiCl ₂	0.3	0.2	0.3	6.6
SG2	HPC	NiCl ₂	0.15	0.2	4	9.4
SG3	HPC	CoCl ₂	0.15	0.2	4	9.4
SG4	HPC	-	0.15	-	7.7	9.4
SG5	CA	CoBr ₂	0.3	0.1	0.2	5.3
SG6	CA	CoBr ₂	0.3	0.1	4	4.9
SG7	CA	CoBr ₂	0.4	0.1	5.5	5.1
SG8	CA	CoBr ₂	0.15	0.2	3.9	5.7
SG9	CA	CoBr ₂	0.3	0.2	8	4.4
SG10	CA	CoBr ₂	0.3	0.2	0.1	6.6
SG11	CA	CoBr ₂	0.3	0.2	0.1	5
SG12	CA	CoBr ₂	0.3	0.2	0.1	4.5
SG13	CA	CoBr ₂	0.4	0.2	0.2	5.1
SG14	CA	CoBr ₂	0.15	0.4	6.6	5.2
SG15	CA	Co(NO ₃) ₂	0.3	0.2	0.3	4.5
SG16	CA	Co(NO ₃) ₂	0.15	0.2	3.9	5.7
SG17	CA	CoCl ₂	0.3	0.2	0.3	4.5
SG18	CA	CoCl ₂	0.3	0.2	0.4	5
SG19	CA	CoCl ₂	0.15	0.2	4	5.7

Table A2 Time required to form gels in the presence of HPC

Sample	Salt	metal /HPC weight ratio	Time of gelation	Appearance of gels
SG1	NiCl ₂	0.2	48h in oven + 60 days	Transparent,monolith
SG2	NiCl ₂	0.2	6 days in oven	Transparent,monolith
SG3	CoCl ₂	0.2	6 days in oven	Transparent,monolith
SG4	-	-	7 days in oven	Transparent,monolith

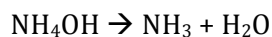
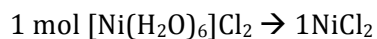
Table A3 Characteristics of gels prepared in the presence of CA

Sample	Salt	metal/CA weight ratio	Time of gelation	Appearance of gels
SG5	CoBr ₂	0.1	15 days in oven	Opaque syneresis
SG6	CoBr ₂	0.1	15 days in oven	Opaque
SG7	CoBr ₂	0.1	23 days in oven	Opaque, syneresis
SG8	CoBr ₂	0.2	5 days in oven	Opaque, syneresis
SG9	CoBr ₂	0.2	8 days in oven	Opaque, syneresis
SG10	CoBr ₂	0.2	20 days in oven	Opaque, syneresis
SG11	CoBr ₂	0.2	15 days in oven	Opaque, syneresis
SG12	CoBr ₂	0.2	5 days in oven	Opaque, syneresis
SG13	CoBr ₂	0.2	14 days in oven	Opaque, syneresis
SG14	CoBr ₂	0.4	7 days in oven	Opaque, syneresis
SG15	Co(NO ₃) ₂	0.2	60 days + 10 days in oven	Opaque, syneresis
SG16	Co(NO ₃) ₂	0.2	26 days in oven	Opaque
SG17	CoCl ₂	0.2	60 days + 10 days in oven	Opaque
SG18	CoCl ₂	0.2	60 days	Opaque
SG19	CoCl ₂	0.2	60 days	Opaque

Table A4 Comparison of acid and basic catalyst protocol

	HCl protocol	NH ₄ OH protocol
Precursor/SiO ₂ weight ratio	0.3	0.3
metal / precursor weight ratio	0.2	0.2
HCl (mL)	0.3	0
NH ₄ OH (mL)	0	0.97

Calculation of quantity of NH₄OH



NH₄OH = 0.91 g/cm³ (25 % wt)

For 2.5 mL of NiCl₂

$$2.5 \times 10^{-3} \text{ L} \times 0.42 \text{ mol/L} = 1.05 \times 10^{-3} \text{ mol} = 6.3 \times 10^{-3} \text{ mol}$$

$$6.3 \times 10^{-3} \text{ mol} \times 35.04 \text{ g/mol} = 0.221 \text{ g}$$

$$\frac{0.221 \text{ g}}{0.25} = 0.883 \text{ g}$$

$$\frac{0.883 \text{ g}}{0.91 \text{ g/mL}} = \mathbf{0.97 \text{ mL}}$$

Title: Synthesis of nanostructured Ni(Co)/C/SiO₂ composites from cellulose derivatives through sol-gel approach



Task 1: Bibliographic research

Task 2: Synthesis of cellulose derivative/silica gels containing Ni(II) and Co(II) salts by sol-gel technique

Task 3: Synthesis of porous Ni(Co)/C/SiO₂ composites by carbonization of cellulose derivative/silica xerogels containing Ni(II) and Co(II) salts;

Task 4: Analysis of synthesized materials with SEM, XRD, TGA and low temperature nitrogen sorption;

Task 5: Report.

Figure A1 Timeline

Table A5 Characterization methods performed in each sample

Sample	Carbon precursor	Salt	Conditions	N ₂ Adsorption	SEM	XRD	TGA	FTIR
SG1	HPC	NiCl ₂	HPC/SiO ₂ = 0.3 metal/HPC = 0.2 H ₂ O/TEOS = 0.3	X	X	X		X
SG2	HPC	NiCl ₂	HPC/SiO ₂ = 0.15 metal/HPC = 0.2 H ₂ O/TEOS = 4	X				X
SG3	HPC	CoCl ₂	HPC/SiO ₂ = 0.15 metal/HPC = 0.2 H ₂ O/TEOS = 4	X				X
SG4	HPC	-	HPC/SiO ₂ = 0.15 H ₂ O/TEOS = 7.7	X	X		X	X
SG5	CA	CoBr ₂	HPC/SiO ₂ = 0.3 metal/HPC = 0.1 H ₂ O/TEOS = 0.2	X				
SG6	CA	CoBr ₂	HPC/SiO ₂ = 0.3 metal/HPC = 0.1 H ₂ O/TEOS = 4	X				
SG7	CA	CoBr ₂	HPC/SiO ₂ = 0.4 metal/HPC = 0.1 H ₂ O/TEOS = 5.5	X				
SG8	CA	CoBr ₂	HPC/SiO ₂ = 0.15 metal/HPC = 0.2 H ₂ O/TEOS = 4	X	X			X
SG9	CA	CoBr ₂	HPC/SiO ₂ = 0.3 metal/HPC = 0.2 H ₂ O/TEOS = 8	X		X		
SG10	CA	CoBr ₂	HPC/SiO ₂ = 0.3 metal/HPC = 0.2 H ₂ O/TEOS = 0.1	X				X

Sample	Carbon precursor	Salt	Conditions	N ₂ Adsorption	SEM	XRD	TGA	FTIR
SG11	CA	CoBr ₂	HPC/SiO ₂ = 0.3 metal/HPC = 0.2 H ₂ O/TEOS = 0.1	X	X			X
SG12	CA	CoBr ₂	HPC/SiO ₂ = 0.3 metal/HPC = 0.2 H ₂ O/TEOS = 0.1	X	X	X		
SG13	CA	CoBr ₂	HPC/SiO ₂ = 0.4 metal/HPC = 0.2 H ₂ O/TEOS = 0.2	X		X		X
SG14	CA	CoBr ₂	HPC/SiO ₂ = 0.15 metal/HPC = 0.4 H ₂ O/TEOS = 6.6	X		X		
SG15	CA	Co(NO ₃) ₂	HPC/SiO ₂ = 0.3 metal/HPC = 0.2 H ₂ O/TEOS = 0.3	X		X		X
SG16	CA	Co(NO ₃) ₂	HPC/SiO ₂ = 0.15 metal/HPC = 0.2 H ₂ O/TEOS = 4	X	X	X		X
SG17	CA	CoCl ₂	HPC/SiO ₂ = 0.3 metal/HPC = 0.2 H ₂ O/TEOS = 0.3	X	X			X
SG18	CA	CoCl ₂	HPC/SiO ₂ = 0.3 metal/HPC = 0.2 H ₂ O/TEOS = 0.4	X	X	X		X
SG19	CA	CoCl ₂	HPC/SiO ₂ = 0.15 metal/HPC = 0.2 H ₂ O/TEOS = 4	X				X